Final report, K119417, KCa1.1 channel expression and function in cancer

The main goal of the project was to investigate the expression pattern of ancillary β subunits of the big conductance KCa1.1 potassium channel on various cancer cell types as well as to study whether changes in the expression of KCa1.1 subunits regulate the invasive and metastatic potential of cancer.
The figure below summarizes our major achievements with more detailed description below:

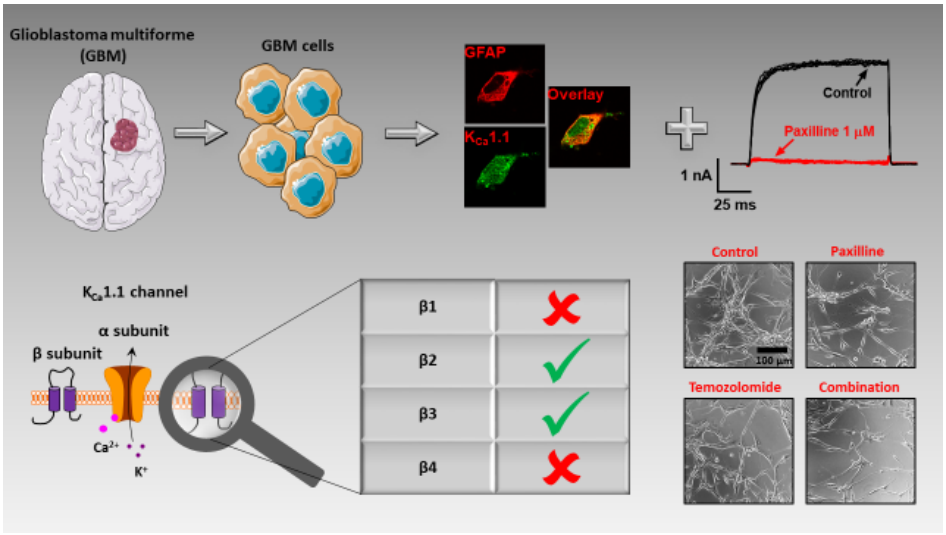

We have examined a known invasiveness factor of glioblastoma multiforme (GBM) cells, the $K_{Ca}1.1$ channel. Our results indicate that the β3 is the dominant auxiliary subunit associated with the channel. As this channel is more dominant in G_2/M phase and is playing role in the chemosensitivity, we propose the $K_{Ca}1.1$ channel as a supportive drug target in GBM chemotherapy.

Specific aim 1: to determine if pathological KCa1.1 beta subunit phenotypes are associated with glioblastoma multiforme, prostate cancer and small cell lung cancer.

1.1. We showed the presence of the KCa1.1 pore forming subunit in both in primary glioblastoma cells and in U-87 glioblastoma cell lines. This is supported by the presence of an intracellular free Ca^{2+} dependent current in the U-87 cells (Fig 1A), the characteristic current-voltage relationship in both cells types (Fig 1B) and the pharmacology of the current, i.e., very significant reduction of the whole-cell current in the presence of 1 uM paxilline, the inhibitor of the KCa1.1 channel (Fig 1 D and E). The expression KCa1.1 in primary glioblastoma was confirmed using confocal microscopy (Fig. 1 C).

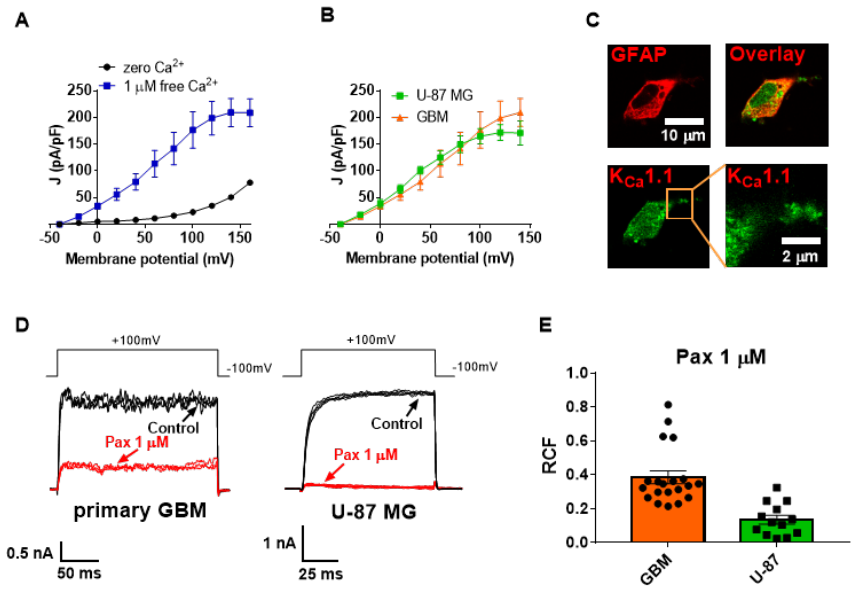

Figure 1. The main ion channel in glioblastoma cell membrane is $K_{Ca}1.1$

A) Current density-voltage relationship of whole-cell currents in primary glioblastoma cells. Current densities (J, pA/pF) at the indicated membrane potentials were calculated by dividing the peak current by the cell membrane capacitance. Data were obtained with intracellular solutions containing zero Ca^{2+} (n=11) or 1 μM Ca^{2+} (n=5). **B)** Current density-voltage relationship of whole-cell currents in primary glioblastoma cells (GBM, orange, n=5) and in the U-87 MG glioblastoma cell line (U-87, green, n=5). **C)** Confocal microscopy images of a primary GBM cell. GFAP (top left) was labeled with anti-mouse Alexa 555, the KCa1.1 alpha subunit was labeled with anti-rabbit Alexa 647, the overlay of the two images is in the top right. The bottom right panel depicts the punctate staining pattern of

KCa1.1 with higher magnification. **D)** Representative whole-cell current traces in a primary glioblastoma cell (GBM, left) and in an U-87 cell. Currents were evoked by repeated depolarizations to +100 mV from a holding potential of -100 mV (see voltage pulse on the top) in control extracellular solution (black) and upon reaching equilibrium block in the presence of 1 μM paxilline application (red). **E)** Remaining current fractions (RCF=I/I_0 were I_0 and I are the peak currents in the absence and in the presence of the inhibitor, respectively) of the outward currents in primary glioblastoma (GBM) and U-87 cells in the presence of 1 μM paxilline. Black symbols indicate RCF values obtained in individual cells. Throughout the figure data points (or bar heights) are mean ± SEM for the indicated number of experiments.

1.2 We showed that KCa1.1 β3 is the main auxiliary subunit associated to the channel in glioblastoma. This statement is supported by the following lines of evidence: we demonstrated that arachidonic acid (AA) activates the current in both primary glioblastoma and U87 cells, which point indicate that K_{Ca}1.1 is assembled with the β2 or β3 subunits (Fig 2B), the presence of the lithocholic acid-sensitive β1-complexed channel is seen in U-87 cell only (Fig 2A). The lack of inactivation of the whole-cell current eliminates the presence of β2-complexed KCa1.1 (Fig. 2 C) and the sensitivity of the whole -cell current to Iberiotoxin (IbTx) eliminates the presence of the β4 subunits in the complex (this subunit would otherwise impede toxin binding to the channel, Fig 2D). The dominant presence of the β3 subunit transcripts was shown using PCR (Fig 3A). We also showed using siRNA methods that silencing β1, β2 or β3 subunit expression separately (Fig 3B) resulted in AA and LCA sensitivities of the currents that are consistent with β3 subunit expression: the currents responses to activators were insensitive to silencing β1 or β2, however, β3 silencing markedly reduced the response of the whole-cell currents to AA (Fig 3C-E).

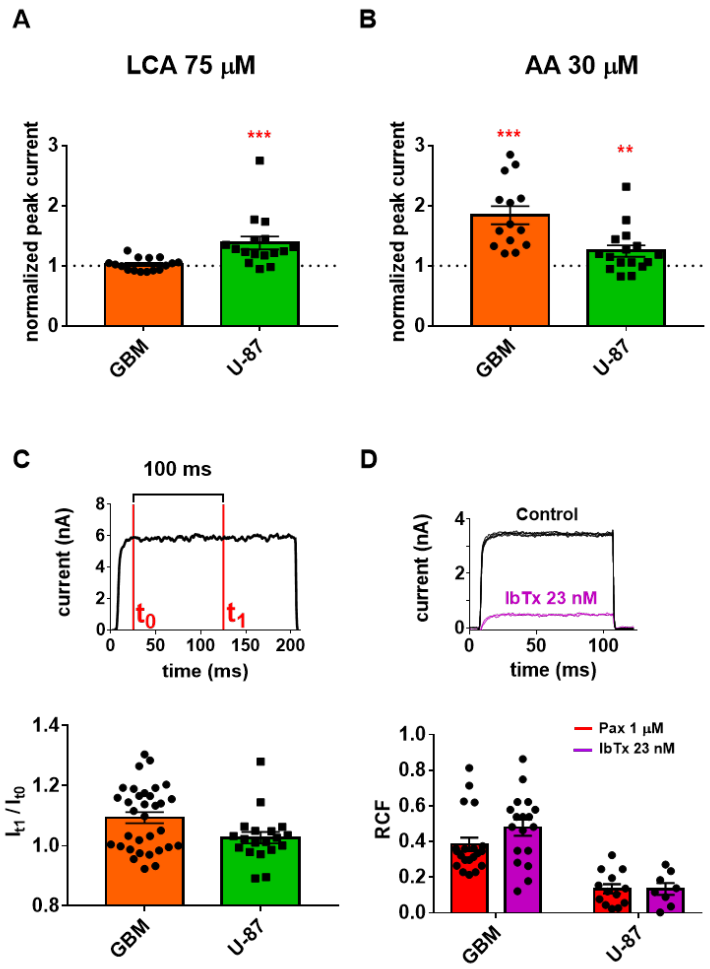

Figure 2. Pharmacological modulators affect β subunit associated K_{Ca}1.1 channels in glioblastoma.
A) The effect of lithocholic acid (LCA, 75 μM) on primary GBM (orange bar, n=16) and U-87 MG cells (green bar, n=16). The current recorded during LCA application was normalized to the current recorded with control solution (dotted line). **B)** The effect of arachidonic acid (AA, 30 μM) on primary GBM (orange bar, n=14) and U-87 MG (green bar n=16) cells. The current recorded during AA application was normalized to the current recorded with control solution (dotted line). **C)** Channel inactivation in a 100 ms time interval was determined by the current ratio I_{t1}/I_{t0}, where t_0 was the current amplitude at the beginning (20 ms after voltage pulse), and t_1 was the current amplitude at the end of the 100 ms time interval. for primary GBM cells (orange, n=33) and for U-87 cells (green bar, n=19) **D)** The effect of iberiotoxin (IbTx, 23 nM, purple bar, n=8) and paxilline (Pax, 1 μM, red bar, n=13) on the K_{Ca}1.1 current in primary GBM and in U-87 cells. Black symbols indicate remaining current fraction (RCF) values obtained in individual cells. RCF is defined in the text and in the legend to Fig. 1. Data represent mean ± SEM, **p<0.01, ***p<0.001

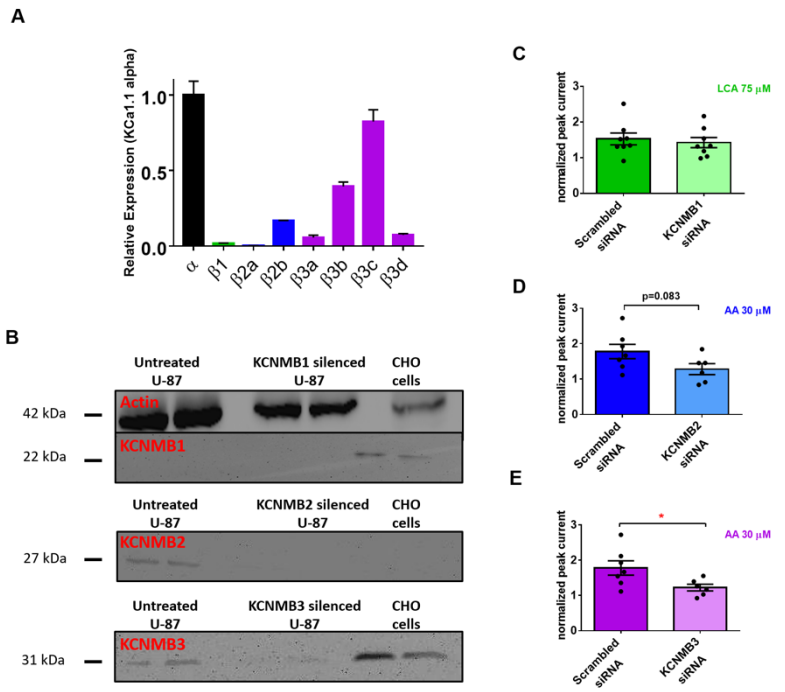

Figure 3. Gene silencing confirms dominant KCa1.1 β3 subunit expression in U-87 GBM.
A) Results of qPCR experiments assessing the relative expression of the beta subunits (black bar) in the U-87 MG cell line. β1, β2 and β3 mRNA levels divided by the expression of the K_{Ca}1.1 channel α-subunit are represented with green, blue and purple bars respectively (N=3, n=3). **B)** Western blot of the untreated and gene silenced U-87 cells. The populations were tested in duplicate, the left two lanes are the untreated U-87 cells and the right two lanes are CHO cells. The middle lane pairs are for the KCNMB1, KCNMB2 and KCNMB3 silenced populations, from top to bottom, respectively. The thick band in the top box at 42 kDa corresponds to actin and the 22 kDa marker to KCNMB1. In the second box (middle) the KCNMB2 bands are shown (27 kDa marker), and in the third box (bottom) the KCNMB3 band are shown (31 kDa marker). (C to E) Pharmacological studies after gene silencing ($N_{Silence}$=3). Whole-cell currents were recorded as in Fig1D, peak currents were measured and normalized peak current was calculated as in Fig 2A and B. **C)** Effect of 75 μM LCA on control scrambled siRNA (dark green bar, n=8) and on KCNMB1 siRNA transfected (light green bar, n=8) U-87 MG cells. **D)** Effect of 30 μM AA on the KCNMB2 (light blue bar, n=6), and **E)** on the KCNMB3 siRNA treated cells (light purple bar, n=6), compared to the scrambled siRNA transfected groups (dark blue and dark purple bars respectively, n=7). Throughout the figure, bar heights are mean ± SEM for the indicated number of experiments, *p<0.05

We used our expertise gained this study to determine the explore arachidonic-acid sensitive ion channels in other cells as well, e.g. mesenchymal stem cells with significant KCa1.1 expression to gain knowledge about the pleiotropic effects of arachidonic-acid treatment. (**Meszaros et al, Sci. Rep, 2020**). Moreover, we investigated the mRNA expression of KCa1.1 β subunits on the prostate cancer cell line PC-3, where we found marked expression of β1 as well as expression of β3. On these cells, we only found KCa1.1 expression without any signs of chloride or sodium channels. Interestingly, the pharmacological evaluation of the whole cell currents indicates a potassium channel phenotype similar to the U87-MG cell line.

Specific aim 2: To study if changes in KCa1.1 α and β subunit expression regulate cancer invasion and metastatic potential

This part of the project aims to describe the functional role of KCa1.1 and its auxiliary β subunits in the migration, invasion and Ca^{2+} signaling of cancer cells.

2.1 First, we established that KCa1.1 is a key determinant in regulating Ca^{2+} signaling in glioblastoma and showed, that the carbachol-induced Ca^{2+} signal in U-87 was sensitive to the inhibition of KCa1.1 by paxilline (Fig 4 A,B). The pharmacological evidence was supported by gene silencing ones, i.e., siRNA mediated silencing of the KCa1.1 gene (KCNMA1) resulted in an impaired Ca^{2+} response to carbachol. More interestingly, silencing of the gene encoding the β3 subunit (KCNMB3) resulted in reduction of the peak Ca^{2+} responses comparable to silencing of KCa1.1 itself. This indicates the primary role of KCa1.1 and its β3 subunit in the regulation of Ca^{2+} signaling induced by carbachol. As an additional benefit, the technical development in this project (building and learning Ca^{2+} imaging using the Visitron system) was also used by Vörös et al. (**Vörös et al, Int. J. Mol.Sci, 2021)** to gain insight into Ca^{2+} signaling in T cells.

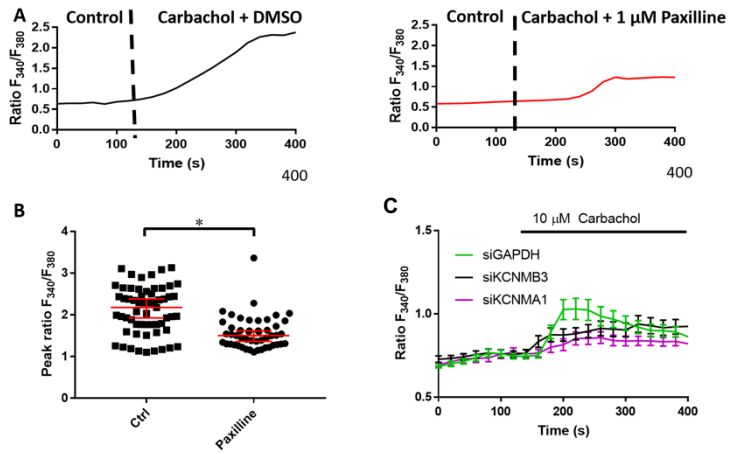

Fig. 4. $K_{Ca}1.1$ β3 is involved in the Ca^{2+}-response of U87-MG cells
A) Representative intracellular Ca^{2+} measurements, where F_{340}/F_{380} ratio is directly proportional to the intracellular Ca^{2+} concentration. Dotted line shows start of carbachol. superfusion after 2 min superfusion with control [(left panel: black line, 0.1% DMSO in 10 µM carbachol-containing solution, N=5, n=120); or in combination with paxilline (right panel: red line, 10 µM carbachol + 1 µM paxilline, (N=5, n=91). **B)** Peak of the 10 µM carbachol-induced F_{340}/F_{380} ratio (see A and B for details) of control superfused cells (n=59, N=3) and 1 µM paxilline-treated cells (n=49, N=3). **C)** Carbachol-elicited intracellular Ca^{2+} response of cells after silencing of GAPDH (green, siGAPDH, N=3, n=39 (F_{340}/F_{380}= 1.1 ± 0.06), $K_{Ca}1.1$ (purple, siKCNMA1, N=3, n=51 (F_{340}/F_{380}= 0.8 ± 0.04) and $K_{Ca}1.1$ beta 3 (black, siKCNMB3, N=3, n=30 (F_{340}/F_{380}= 0.9 ± 0.04)). In C) and D) data are mean ± SEM for the indicated number of experiments, *p<0.05.

2.2 As cytosolic Ca^{2+} fluctuates during the cell cycle, and K^+ channels are expressed in a cell cycle-dependent manner, we aimed at testing whether the $K_{Ca}1.1$ β3 subunit regulates the cell cycle of glioblastoma cells. We generated non-synchronized, G_0 synchronized (starvation-induced, also labeled as G_0/G_1 as flow cytometry can identify this population) and M synchronized (arrested in M phase by colchicine treatment, also labeled as G_2/M, based on flow cytometric identification) U-87 glioblastoma cells and studied the electrophysiological and pharmacological properties of the whole-cell currents using patch-clamp. Fig. 5A shows a marked increase in the magnitude of the whole-cell current in a representative M phase synchronized cell as compared to control (non-synchronized, untreated) and G_0 synchronized one (Fig. 5A). As cell volume and cell surface are can also change during the cell cycle, we also determined peak current normalized to cells capacitance (current density, J) and showed that the J values are significantly larger in the M phase synchronized cells as compared to control and G_0 phase synchronized ones at depolarized test potentials (Fig. 5B).

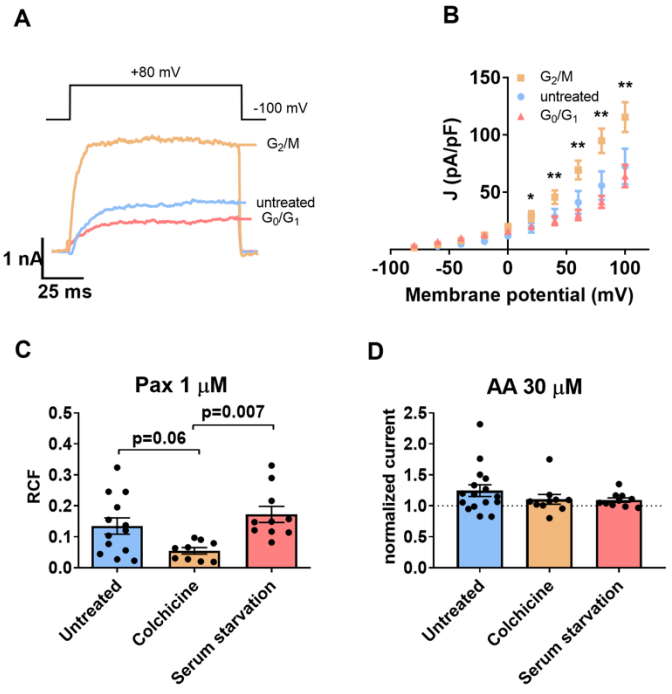

Figure 5. $K_{Ca}1.1$, but not the β3 subunit shows cell cycle-dependent function
A) Representative patch-clamp traces of the serum starved (red), colchicine-treated (orange) and untreated (blue) populations. Currents were recorded at +80 mV depolarizing pulse with 1 µM free Ca^{2+} in the pipette-filling solution. **B)** Peak current density (J, pA/pF) as a function of membrane potential (mV) was calculated for n=18 control (blue), n=18 colchicine-treated (orange) and n=7 starving cells(red) **C)** Effect of 1 µM paxilline on the whole cell currents in untreated (n=13), colchicine-treated (n=9) and starving cells (n=10). Black symbols indicate RCF values obtained in individual cells, RCF was calculated as in Fig 1). **D)** The effect of 30 µM AA on the normalized current in untreated (n=16), colchicine-treated (n=10) and starving cells (n=10). Bars indicate the current amplitude measured with AA superfusion normalized to the current amplitude measured with control solution. Throughout the figure data points (or bar heights) are mean ± SEM for the indicated number of experiments, *: p<0.05; **: p<0.01.

Application of paxilline confirmed that the main component of the whole-cell currents is $K_{Ca}1.1$ (Fig. 5C) in all studied phases of the cell cycle. On the other hand, the increase in the whole-cell current induced by 30 µM AA was similar in all groups (Fig. 5D). Together, these results indicate that $K_{Ca}1.1$ function is increased after M phase synchronization, without alterations in the β3 subunit-dependent modulation in the K^+ current.

2.3 Motivated by our results that colchicine-synchronized U-87 MG have increased $K_{Ca}1.1$ current density, we wanted to exploit this phenotype by testing whether $K_{Ca}1.1$ inhibition potentiates temozolomide (TMZ) chemotherapy. We investigated the short-term effects of TMZ and the $K_{Ca}1.1$ inhibitor separately or in combination over the first few hours of treatment (~6h) using time-lapse video microscopy, where we evaluated the migration of U-87 MG cells. As shown in Fig. 6A and 6B, we found that TMZ (500 µM) alone does not reduce the velocity of two-dimensional spontaneous cell migration over 6 h as compared to control. In contrast, paxilline alone and in combination with temozolomide reduced cell migration velocity similarly, by ≈ 50%. Moreover, as Fig 6C and D shows paxilline has an additive effect to temozolomide in reducing the viability of U-87 MG cells, but his evolves over the course of days rather than hours.

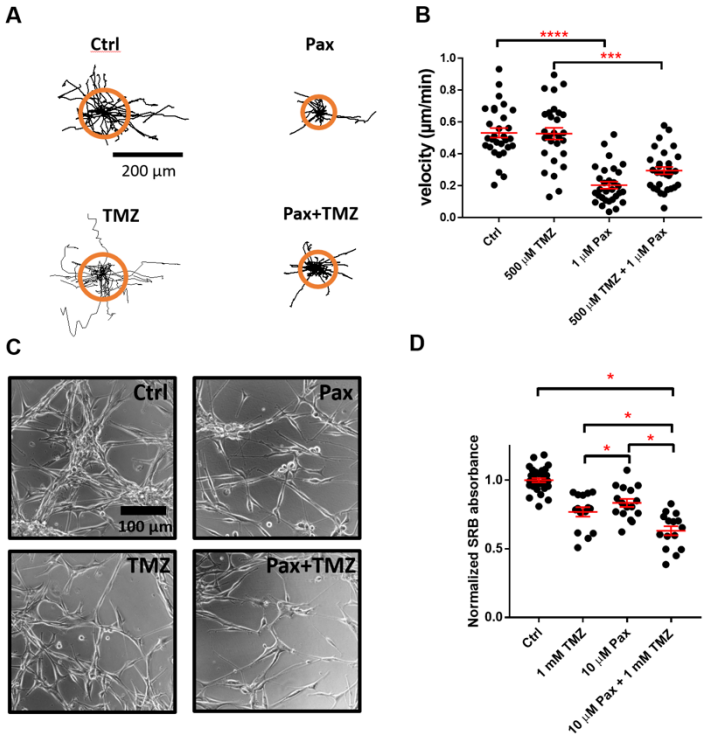

A) Migration trajectories of U-87 MG cells (black lines) over 6h treated with 0.1% DMSO (Ctrl), 500 µM temozolomide (TMZ), 10 µM paxilline (Pax) and combined 10 µM paxilline + 500 µM temozolomide (Pax+TMZ) treatment. Orange circle indicates the mean start-to-end translocation. **B)** Scatter plot shows quantification of migration velocities (µm/min) of U-87 MG cells depicted in panel (A) (N=3, n=30). **C)** Representative phase-contrast microscopy images of U-87 MG cells treated for 48h with 10 µM Pax and/or 1 mM TMZ, as indicated on the panels **D)** Cell viability was determined by sulforhodamine B (SRB) assay after 48 h by normalizing the SRB absorbance in the treatment group to the SRB absorbance upon control (Ctrl) treatment (N=4, n=32) after 48 h paxilline and/or temozolomide (N=4, n=15) treatment, *p< 0.05, ***p<0.001, ****p<0.0001

In summary, we found using molecular biology, patch-clamp electrophysiology and intracellular Ca^{2+} -measurements that $K_{Ca}1.1$ β2 and β3 subunits are functionally expressed in GBM cells, independently from the cell cycle. We also found that the outward ionic currents were significantly higher in cells arrested in the cell cycle M phase by colchicine. Moreover, the $K_{Ca}1.1$ blocker paxilline potentiated the effect of chemotherapeutic agent, temozolomide. Based on these results, we propose a tissue specific inhibition of the $K_{Ca}1.1$ channel in combination with cell-cycle specific chemotherapy as an effective treatment for glioblastoma patients.

As for regulation of the Ca^{2+} signaling by K^+ channels, we have elaborated a novel model where the interplay of the ion channels leads to an oscillatory membrane potential response of non-excitable cells **(Papp et al, Int. J. Mol. Sci, 2020, Nagy et al, Biophys J, 2018).** To facilitate pharmacological separation of ion channels with different subunit composition and identify more specific K^+ channel inhibitors we tested various animal venoms and pure peptides

isolated/recombinantly expressed in cooperation with our foreign collaborators in Mexico and Australia (**Krishnarjun et al, J. Struct. Biol, 2020; Luna-Ramirez et al, Mol. Pharmacol, 2020; Jin et al, Ins. Biochem. Mol. Biol. 2020; Tajti et al, Biochem Pharmacol, 2020, Alvarado et al, Front. Pharmacol, 2021, Borrego et al, Pharmaceuticals, 2021, Krishnarjun et al, J. Struct. Biol, 2021, Reddair at al, Toxicon, 2021, Varga et al, Biologia Futura, 2021**). Targeting KCa1.1 having different subunit stoichiometries might be possible with novel peptide inhibitors that have blocking mechanism that is different from the well-known pore blocker or gating modifier peptides. We have made a very significant advance in this during the last year by describing a peptide inhibitor that induced block of the current by enhancing the inactivation of the ion channels. This paper has been published in cooperation with the Weitzman Institute in Israel (**Karbat et al, PNAS, USA. 2019**). Two of our papers regarding ion channel biophysics has contributed to the development of this new group of toxin inhibitors of ion channels, in which deep biophysics of ion channel gating and molecular interactions regulating gating were described (**Szanto et al, J. Gen. Physiol, 2020, Szanto et al, J. Gen.Physiol, 2021**). During the completion of the research project we also made very significant advance in establishing recombinant production of peptide toxins in my laboratory (**Naseem et al, Front. Pharmacol. 2021)**. It is also clear by now that the membrane microenvironment will be a key determinant in understanding KCa1.1 function in various tissues including cancer cells. In that respect we also made very significant progress in understanding the effect of membrane composition on the operation of ion channels in the plasma membrane with special focus on cholesterol **(Balajthy et al, Current topics in membranes, 2018, Zakany et al, BBA- Molecular and Cell Biology of Lipids, 2019, Zakany et al, BBA- Molecular and Cell Biology of Lipids, 2020, Kovacs et al, Front. Mol. Biosci, 2021**). The technical developments of the current project were also applied in determining the contribution of auxiliary subunits to Kv1.3 function (**Vallejo-Gracia et al, Sci. Rep., 2021**), and the project significantly contributed to the refinement of cell isolation techniques (**Tajti et al, 2021).**

The most important findings of the project are summarized in a full-length manuscript to be submitted in January 2022 in a D1 journal (see attached manuscript). The PI of the project was invited to present the results on two international conferences (51th Annual Scientific Meeting of the Hungarian Medical Association of America, 2019.10.27-2019.11.01, Sarasota, Fl., USA; 2nd International Cancer & Ion Channels Congress,, Izmir, Turkey, 2019.09.20-2019.09.25).

There are 24 papers already published in peer reviewed journals and supported by the current grant, of these 5 are D1/Q1 and 15 are Q1, with a cumulative impact factor of 105.37. As a consequence of our involvement in understanding the role of ion channels in malignancies my laboratory was invited to the H2020 Marie Sklodowska Curie Innovative Training Network, project ID: 813834: pH and Ion Transport in Pancreatic Cancer: pHioniC, which is now running and supports fully an international PhD student in my lab along with bench fees. We have already published a significant review as part of the consortium in the topic of ion channels in cancer (**Hofschröer et al, Frontiers in Pharmacol., 2021.**). Moreover, a postdoc from my lab was invited during the grant period to work on ion channel in cancer in Münster, Germany, where he is now close to habilitation and expected to return to my department and start his own lab with international grants that are spinning off the currently reported proposal. The Covid-19 situation has hampered the achievement of some of our goals, especially obtaining tissue samples for prostate and lung cancer and thus, we could not complete the characterization of the auxiliary subunits of KCa1.1 in these tissue samples. Although we have a shortcoming on this side, we are convinced that outreach from this grant to other projects, the start of a new EU H2020 financed one and the significant amount of publications with the support of this grant may compensate for the shortcoming, especially considering the numerous technical and strategic developments (e.g. Ca^{2+} imaging and recombinant peptide production).

Beta 3 is the main auxiliary subunit associated with the $K_{Ca}1.1$ channel in glioblastoma

Adam Feher[1#], Zoltán Pethő[1,2#], Tibor G. Szanto[1], Álmos Klekner[3], Gabor Tajti[1], Gyula Batta[4], Tibor Hortobágyi[5,6], Zoltan Varga[1], Albrecht Schwab[2] and Gyorgy Panyi[1*]

[1]*Department of Biophysics and Cell Biology, Faculty of Medicine, University Debrecen, Debrecen, Hungary*
[2]*Institute of Physiology II, University Münster, Münster, Germany*
[3]*Department of Neurosurgery, Faculty of Medicine, University Debrecen, Debrecen, Hungary*
[4]*Department of Genetics and Applied Microbiology, University Debrecen, Debrecen, Hungary*
[5]*Institute of Pathology, Faculty of Medicine, University of Szeged, Szeged, Hungary.*
[6]*Department of Neurology, Faculty of Medicine, University Debrecen, Debrecen, Hungary*

*Corresponding author, Tel.: +36 52 411 717 / 65617, E-mail: panyi@med.unideb.hu
# These authors contributed equally to the manuscript

Running title: $K_{Ca}1.1$ functions together with β subunits in glioblastoma

Abbreviations: GBM - glioblastoma multiforme; PAX – paxilline; LCA – lithocholic acid; AA – arachidonic acid; Ibtx – iberiotoxin; TMZ – temozolomide; gBK – glioma BK; GFAP – glial fibrillary acidic protein; RCF – remaining current fraction; PI – propidium iodide; Ach – acethylcholine

---

Abstract

Glioblastoma Multiforme (GBM) is the most aggressive glial cancer, where state-of-the-art treatment procedures are often ineffective. Therefore, it is crucial to study the molecules involved in GBM cell homeostasis, such as ion channels in order to develop new therapeutic and diagnostic options. Even though $K_{Ca}1.1$ is known to be expressed in GBM tumor cells and is associated with tumor radiosensitivity, it is not known whether it is involved in chemosensitivity. Moreover, the auxiliary subunits linked to these channels in GBM are largely unknown. Here, we aimed to characterize the $K_{Ca}1.1$ β subunit composition in both primary tumor cells and in the glioblastoma cell line U-87 MG.

We found that $K_{Ca}1.1$ $\beta 2$ and $\beta 3$ subunits are functionally expressed in GBM cells, independently from the cell cycle, using molecular biology, patch-clamp electrophysiology and intracellular Ca^{2+}-measurements. We also found that the outward ionic currents were significantly higher in cells arrested in the cell cycle M phase by colchicine. Moreover, the $K_{Ca}1.1$ blocker paxilline potentiated the effect of chemotherapeutic agent, temozolomide. Based on these results, we propose a tissue specific inhibition of the $K_{Ca}1.1$ channel in combination with cell-cycle specific chemotherapy as an effective treatment for glioblastoma patients.

Keywords: Glioblastoma, $K_{Ca}1.1$ channel, Regulatory subunit, Patch-clamp electro- physiology, Ca^{2+} imaging

Graphical abstract

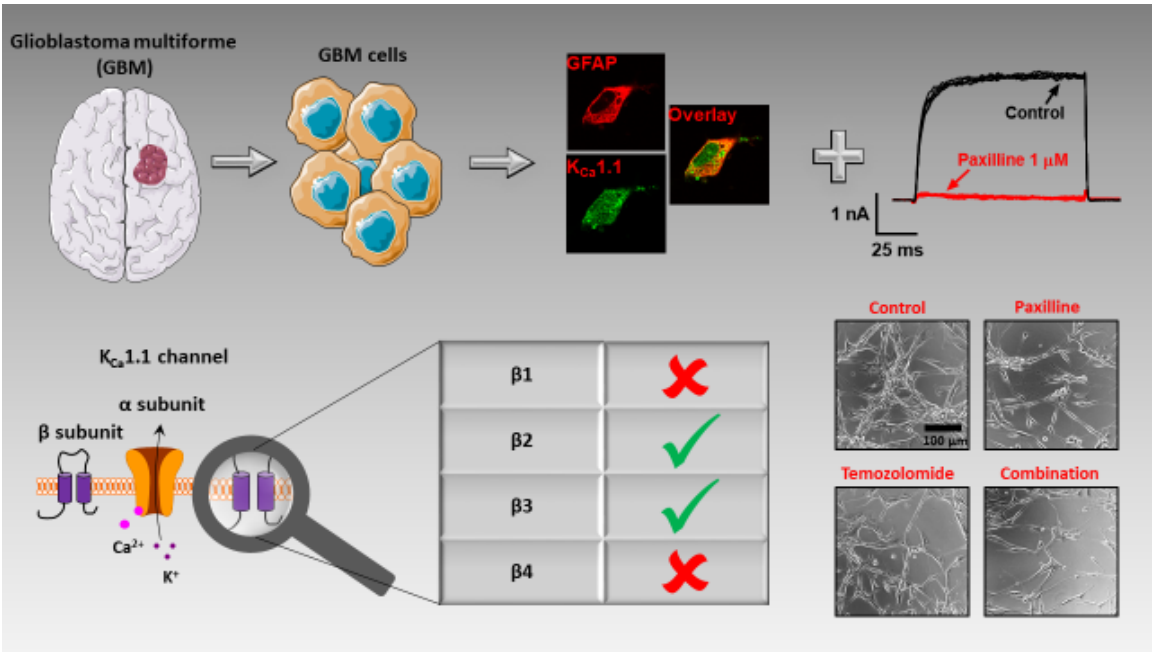

We have examined a known invasivity factor of glioblastoma multiforme (GBM) cells, the $K_{Ca}1.1$ channel. Our results indicate that the β3 is the dominant auxiliary subunit associated with the channel. As this channel is more dominant in G_2/M phase and is playing role in the chemosensitivity, we propose the $K_{Ca}1.1$ channel as a supportive drug target in GBM chemotherapy.

1 Introduction

Glioblastoma multiforme (GBM) is a significant health burden in developed countries with an abysmal long-term survival. In the clinical practice, classical chemotherapeutics, such as the alkylating agent temozolomide are combined with surgery and radiotherapy. Moreover, numerous clinical trials exist aiming to optimize chemotherapy with different treatment combinations, from which some show promising effects [1]. These studies are, however, still limited in number, thus new combination therapies are necessary to tackle the therapeutic challenge GBM imposes.

Ion channels are widely targeted in the therapy of various diseases and there is evidence that they may be promising targets in cancers as well [2,3]. In GBM cells, the Ca^{2+}-dependent K^+ channel $K_{Ca}1.1$ (also known as BK_{Ca}, Slo1 or MaxiK) is expressed as one of the major K^+ channels [4,5], with many of its functions unclear and disputed. Notably, the gBK (short for glioma BK) splice variant of $K_{Ca}1.1$ is involved in the radiosensitivity of glioma cell lines [6]. However, the exact molecular mechanisms of these observations remain unclear to date. Moreover, even though radiosensitivity is altered by $K_{Ca}1.1$, there is only scarce evidence whether channel modulation could potentiate GBM chemosensitivity [7].

The pore-forming alpha subunit of $K_{Ca}1.1$, as that of many other ion channels, is associated with auxiliary subunits. These subunits modify the biophysical characteristics of the channel, responsiveness to pharmacological modulators as well as the membrane expression [8]. Notably, it has been described by Ge et al. using the REpository of Molecular BRAin Neoplasia DaTa (REMBRANDT) glioma database that KCNMB3, the gene coding for the $K_{Ca}1.1$ β3 subunit is expressed in a higher copy number in high-grade gliomas leading to a poorer prognosis compared to tumors expressing KCNMB2, the gene encoding the β2 subunit [9]. Comparably, using the same database, the expression of the α subunit (KCNMA1) is upregulated only in ≈10% of GBM patients, and its overexpression does not correlate with overall patient survival [10]. Since the β3 subunit increases the membrane expression of $K_{Ca}1.1$ and abolishes channel inactivation, we hypothesized that the resulting increased K^+ conductance of GBM cells alters tumor cell physiology in a manner that cells have a more pronounced Ca^{2+} signaling leading to enhanced invasiveness and/or therapy resistance. First, as there are no functional analyses to date regarding the membrane expression of the auxiliary β subunits in GBM, we characterized the β subunits of $K_{Ca}1.1$ in primary patient-derived GBM cells as well as using the cell line U-87 MG. Moreover, we investigated if these auxiliary subunits regulate different functional aspects and downstream effects of $K_{Ca}1.1$ and if $K_{Ca}1.1$ inhibition potentiates GBM chemotherapy.

Materials and Methods

1.1 Glioblastoma cell isolation

Experiments on patient-derived GBM tissue samples were carried out under the approval of the Hungarian Research Ethical Committee (ETT-TUKEB, IV/186- 1 /2022/EKU). Informed consent was obtained for all human subjects involved in this study. Tumor samples were collected from anonymized adult patients during the surgical removal of the glioblastoma and transported for further processing in HBSS (Hank's Balanced Salt Solution) on ice. Next, tissue samples were digested for 30 min in Collagenase type I (Sigma Aldrich, Burlington, MA, USA), and eventually homogenized using a tissue homogenizer and using Pasteur pipettes, as modified from [11]. Lastly, single cell suspension was achieved using a 70 µm cell strainer (Corning, Corning, NY, USA). Single cells were left to adhere for 2 h in DMEM + 10% FCS at 37 ºC and 5% CO_2, then washed 3x with PBS. Cells were incubated in DMEM medium including 10% FCS, 1% glutamate, 1% penicillin-streptomycin and 1% non-essential amino acids for a maximum of three passages. Glioblastoma cell purity was routinely assessed using GFAP immunocytochemistry. Only those glioma populations were used for experiments, where >90% of cells showed clear GFAP positivity.

1.2 Patch-clamp electrophysiology

Whole-cell currents of voltage-clamped cells were recorded by manual patch-clamp electrophysiology according to standard protocols using Axopatch 200B amplifiers connected to a computer and digitized with Digidata 1550B (Molecular Devices, CA, USA). Pipettes were pulled from GC 150F-15 borosilicate glass capillaries (Harvard Apparatus, MA, USA) in five stages with 4-10 MΩ resistance. Immediately before the measurement, the cells were maintained in the recording petri dish in a bath solution consisting of 145 mM Na-aspartate, 5 mM KCl, 1 mM $MgCl_2$, 2.5 mM $CaCl_2$, 5.5 mM glucose, and 10 mM HEPES, pH 7.4. For the recordings, the composition of the solution used in patch pipette (internal solution) was either Ca^{2+}-free (composition: 140 mM KF, 2 $MgCl_2$, 1 mM $CaCl_2$, 10 mM HEPES, 11 mM EGTA, pH 7.22) or contained 1 µM free Ca^{2+} (145 mM K-aspartate, 10 mM EGTA, 10 mM HEPES, 2 mM $MgCl_2$, 8.5 mM $CaCl_2$, pH 7.2). $K_{Ca}1.1$ channel modulators (lithocholic acid, arachidonic acid, iberiotoxin and paxilline) were diluted to the desired concentration (75 µM, 30 µM, 23 nM and 1 µM, respectively) in the bath solution. Solution exchange was achieved by using a gravity-flow system with continuous excess fluid removal. To avoid the changing of junction potentials during solution changes, the reference electrode, placed in a dish containing internal solution, was connected to the bath solution with agar bridge. For the biophysical characterization of the $K_{Ca}1.1$ currents, the cells were depolarized from a holding potential

of -100 mV to +100 mV in +20 mV increments. For the testing of $K_{Ca}1.1$ channel modulators, we used a 100 or 200 ms ramp depolarization protocol from -100 mV to +100 mV. Voltage-clamp data were acquired with pClamp10 (Molecular Devices, CA, USA). In general, currents were low-pass-filtered using the built-in analog four-pole Bessel filters of the amplifiers and sampled at 5 kHz. Before analysis, whole-cell current traces were digitally filtered (five-point boxcar smoothing). Clampfit 10.7 (Molecular Devices, CA, USA) and Graphpad Prism 7 (Graphpad, CA, USA) were used for data display and analysis.

1.3 Immunocytochemistry

For fluorescent detection of $K_{Ca}1.1$ and the glial fibrillic acidic protein (GFAP), we followed standard immunofluorescence protocol as described in [12]. Briefly, primary patient-derived GBM cells were plated onto coverslips after the first passage. After overnight adhesion, cells were washed, then fixed (4% paraformaldehyde + 0.1% Triton-X-100 in PBS) for 20 min at room temperature. After washing and blocking (10% goat serum in PBS) for 1 h at room temperature, cells were labeled with antibodies against $K_{Ca}1.1$ α (1:200 dilution of AB5228; rabbit polyclonal, Merck Millipore, Darmstadt, Germany) and/or GFAP (1:500 dilution of G3893; mouse monoclonal, Sigma Aldrich, Burlington, MA, USA) overnight at 4 ºC. After washing, fluorescent secondary antibodies against mouse (405324, Alexa-555 rabbit polyclonal, Biolegend, CA, USA) and rabbit (A-21244, Alexa-647 goat polyclonal, Invitrogen, MA, USA) were applied at 1:1000 dilution for 2 h at 4 ºC. Lastly, after washing coverslips were mounted onto slides using DAKO mounting medium (Agilent, Santa Clara, CA, USA). Acquisition and qualitative assessment of the stainings was performed at 40x magnification using a confocal microscope (Olympos FV1000). Cells were labelled GFAP positive if the intracellular staining had a typical filamentary phenotype, and KCa1.1 staining was considered positive when it had a punctate membrane staining pattern typical of ion channels [12,13]

1.4 RNA isolation and RT-qPCR

RNA was isolated from primary GBM cells after 24 h of culture as well as from cultured U-87 MG cells using TRIzol™ (Life Technologies, Carlsbad, CA, USA) following manufacturer's instructions. cDNA was generated using the Superscript III™ Reverse Transcriptase kit (Invitrogen, Waltham, MA, USA) with 2 µg of RNA per reaction. RT-PCR was performed using a QuantStudio 3 cycler with PowerUp™ SYBR™ Green Master Mix (Applied Biosystems®/ Thermo Fisher Scientific, Waltham, MA, USA), according to manufacturer´s instructions. Data was evaluated using the QuantStudio Design and Analysis software (Applied Biosystems®/ Thermo Fisher

Scientific, Waltham, MA, USA). Primer sequences are listed in Supp. Table 2.

1.5 siRNA application

The U-87 MG cells were transfected with siRNA according to manufacturer´s instructions by Dharmacon™ (Horizon Discovery, Lafayette, CO, USA). Briefly, cells were transfected in Gibco® Opti-MEM™ medium (Thermo Fisher Scientific, Waltham, MA, USA), containing 2 µl/ml DharmaFECT™ (Horizon Discovery, Lafayette, CO, USA) and 5 µg/ml scrambled siRNA (AccuTarget™ Negative Contol siRNA, Bioneer, Daejeon, South Korea); or 5µg/ml of a mixture (SMARTpool) of ON-TARGETplus siRNA against either GAPDH (siGAPDH) KCNMA1 (siKCNMA1), KCNMB1 (siKCNMB1), KCNMB2 (siKCNMB2) or KCNMB3 (siKCNMB3) for 24 to 48 hours at 37 ºC and 5% CO_2 before patch-clamp and Western blot analysis. Gene silencing was validated using Western Blot (Figure 3B).

1.6 Western Blot

Protein from U-87 MG cells was isolated using TRIS lysis buffer (25 mM mercaptoethanol, 1 µl/ml Tween 20, 10 µl/ml protease inhibitor, 50 mM TRIS base, pH=7.5) and sonication for 30 s. 120 µg of denatured protein sample was loaded into each well of the 12% ProSieve 50 (Lonza, ME, USA) modified acrylamide gel for electrophoresis (80 mV for 20 min then 120 mV for 90 min), followed by transfer onto PVDF membranes (100 mV 90 min). After blocking (5% skim milk powder in 10 mM TRIS-buffered saline) at 4 ºC for 1 h, the blocked membranes were incubated overnight at 4 ºC with 1:1000-fold dilutions of primary antibodies against the $K_{Ca}1.1$ beta subunits or actin: anti-KCNMB1 (nb300-535, rabbit polyclonal, Novus Biologicals, CO, USA), anti-KCNMB2 (MA5-27646, mouse monoclonal, Thermo Fisher Scientific, Waltham, MA, USA), anti-KCNMB3 (ab137041, rabbit monoclonal, Abcam, Cambridge, UK), anti-actin (a2066, rabbit polyclonal, Sigma-Aldrich, MO, USA). After washing three times, blots were incubated 1:10 000-fold diluted secondary anti-mouse (#7076, Cell Signaling Technology, MA, USA) or anti-rabbit antibodies (#7074, Cell Signaling Technology, MA, USA) at 4 ºC for 2 h. Blots chemiluminescence was detected using a commercial detection system (Chemidoc XRS, Bio-Rad, Hercules, CA, USA).

1.7 Cell synchronization and flow cytometry

For metaphase cell synchronization, U-87 MG cells were incubated with 4 µg/ml colchicine (Sigma Aldrich, Burlington, MA, USA)-containing medium for 24 h at 37 ºC and 5% CO_2. To measure the efficacy of synchronization, colchicine-synchronized as well as the untreated U-87 MG cells were permeabilized with 80% ethanol for 20 min at room temperature and stained with 2 µg/ml propidium-iodide (PI) for 10 min at room

temperature for flow cytometry measurements. The data were acquired with BD FacsAria III Cell Sorter (BD Biosciences, NJ, USA). 488 nm excitation laser and 616/23 nm emission filter with 610 long-pass dichroic mirrors were used for event detection. Data was subsequently evaluated with Flowjo V10 software (BD, Franklin Lakes, NJ, USA).

1.8 Intracellular Ca^{2+} measurements

For intracellular Ca^{2+}-measurements, untreated and siRNA-treated U-87 MG cells were loaded with 3 µM Fura-2-AM (Invitrogen, Waltham, MA, USA)-containing HEPES-buffered Ringer`s solution (140 mM NaCl, 5.4 mM KCl, 1.2 mM $CaCl_2$, 0.8 mM $MgCl_2$, 5.5 mM D-glucose and 10 mM HEPES, titrated to pH 7.4) for 20 min at 37 ºC. Next, cells were washed twice with fresh Ringer`s solution and then were visualized using an ionic imaging setup composed of a Zeiss Axiovert 100 inverted fluorescence microscope (Zeiss, Oberkochen, Germany), a high-speed shutter, a polychromator (Visitron Systems, Puchheim, Germany) and a 37 ºC acquisition cabin. Fura-2 excitation wavelengths were 340 nm and 380 nm, corresponding to the Ca^{2+}-loaded and Ca^{2+}-free excitation optima, respectively, whereas fluorescence emission wavelength was recorded at 510 nm. Therefore, the resulting fluorescence ratio of 340nm divided by 380 nm-excited fluorescence intensities (F_{340}/F_{380}) is directly proportional to the intracellular Ca^{2+} concentrations. The cells were kept at 37 ºC during the whole measurement. During the acquisition, cells were initially superfused with control solution (0.1% DMSO in Ringer´s solution) for 2 min, followed by 5 min with either only 10 µM acethylcholine (Ach)-receptor agonist carbachol (carbamylcholine chloride; Sigma Aldrich, Burlington, MA, USA)-containing Ringer´s solution to elicit a Ca^{2+}-signal (described before by [14,15]), or with 10 µM carbachol + 1 µM paxilline containing Ringer´s solution to simultaneously inhibit $K_{Ca}1.1$. Ratios were evaluated with the Visiview 3.0 software (Visitron Systems, Puchheim, Germany), and ultimately, individual F_{340}/F_{380}-curves were visualized using R [16].

1.9 Cell migration studies

Two-dimensional spontaneous cell migration of U-87 MG cells was recorded via time-lapse video microscopy as described before [12]. First, U-87 MG cells were seeded in uncoated 12.5 cm^2 dishes overnight 37 ºC and 5% CO_2 to adhere. Next, the medium was exchanged to either control medium containing 0.1% DMSO, 1 µM PAX-containing medium, 500 µM TMZ-containing medium or both 1 µ µM PAX + 500 µM TMZ containing medium and the dishes were placed back into the incubator for another 30 min to equilibrate with CO_2. Subsequently, cell migration was recorded for 6h in 37 ºC -heated chambers using CMOS cameras at 5 min intervals using the MicroCamLab 3.1

software (Bresser, Rhede, Germany). Finally, individual cell migration trajectories were manually segmented using the Amira 2019.1 software (Thermo Fisher Scientific, Inc., Waltham, MA, USA), from which cell migration velocity was calculated from the cell centroid displacement as a function of time [17].

1.10 Cell viability assay

As a readout for cellular viability, we performed the sulforhodamine-B (SRB) viability assay in 96-well plates, as described by Vichai et al. [18]. Briefly, after 48 h of treatment with either temozolomide (Tocris, Bristol, UK), paxilline, or control (0.1% DMSO in DMEM) at 37 ºC and 5% CO_2, U87-MG cells were fixed with trichloroacetic acid for 60 min on ice. After four washing steps with dH_2O, 0.04% (wt/vol) aqueous SRB solution (Sigma Aldrich, Burlington, MA, USA) was added to each well, followed by an incubation for 60 min at RT. After four washing steps with 1% acetic acid, wells were left to air dry for 5 min. Lastly, 10 mM TRIS-base solution (pH 10.5) was added to each well, followed by 10 min rocking at RT. Absorbance was detected using a spectrophotometer at 546 nm wavelength.

1.11 Statistical analysis

Data are presented as mean ± SEM. Statistical analysis was carried out using Graphpad Prism 7. Following a D'Agostino-Pearson normality test, unpaired Student's t tests or one-way ANOVA were performed with Tukey's post hoc test, in other cases Mann-Whitney or Kruskal-Wallis tests were used. To assess the effect of the used channel modulators we performed Wilcoxon signed-rank tests. Statistical significance was assumed when $p < 0.05$.

2 Results

2.1 $K_{Ca}1.1$ is a prominent K^+ channel in the plasma membrane of glioblastoma cells

First, we validated the functional expression of the $K_{Ca}1.1$ in the membrane of GBM cells in our experimental setting using whole-cell patch-clamp technique and expressed the currents as current density (J=pA/pF), where currents are normalized to the cell membrane capacitance to obtain a cell-size independent parameter. As seen in Fig. 1A, voltage-gated K^+ channel current density in primary GBM cells is markedly increased in the presence of intracellular 1 µM Ca^{2+} (N=3, n=5) compared to Ca^{2+} free intracellular solution (N=5, n=11) which is characteristic of $K_{Ca}1.1$ channels (-40 mV, p=0.52; -20 mV, p=0.0004; 0 mV and above: p<0.0001, Student's t tests). We also observed a further

characteristic feature of the $K_{Ca}1.1$ channel [19], namely that currents activate at much more negative membrane potentials in the presence of intracellular Ca^{2+}. K^+ currents of the glioblastoma cell line U-87 MG (N=3, n=5) show a similar current-voltage (I-V) relationship to primary GBM cells (Fig. 1B) (N=3, n=11); which confirms the suitability of the cell line as a model to study $K_{Ca}1.1$ in GBM. Also, whole-cell currents of primary GBM and U-87 MG cells are potently inhibited by applying 1 µM of the small-molecule blocker paxilline (Pax) (Fig. 1D and 1E) (remaining current fraction, RCF=0.38 ± 0.04, n=20, and RCF=0.13 ± 0.02, n=13). Using immunofluorescence against $K_{Ca}1.1$, we also detected a punctate membrane staining [12,13] on the membrane of GFAP positive GBM cells (Fig. 1C). These results support previous reports that $K_{Ca}1.1$ functions as a major K^+ channel in GBM [4,5,14,20].

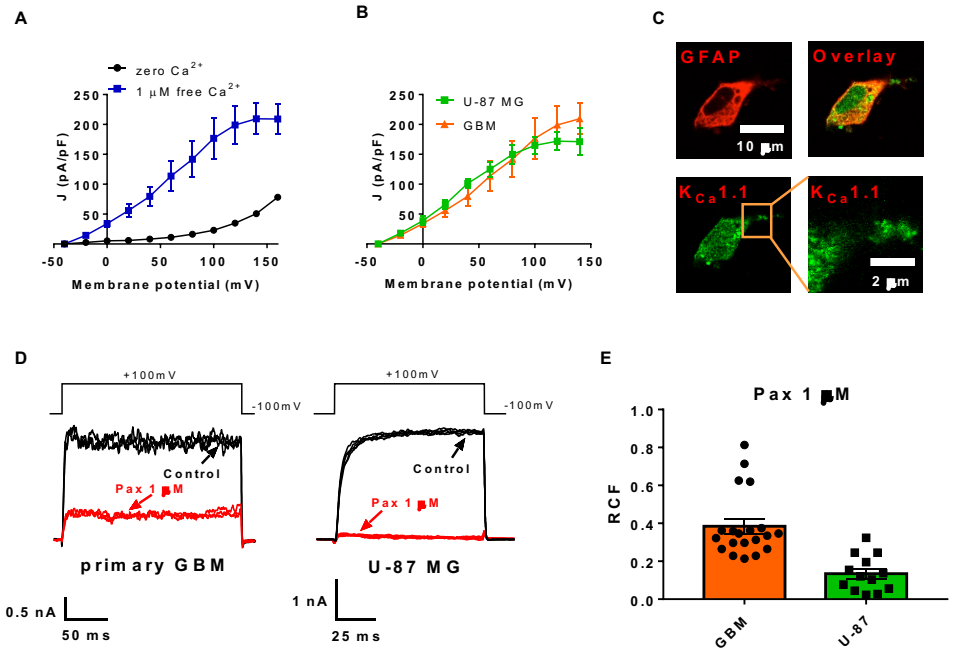

Figure 1. The main ion channel in glioblastoma cell membrane is $K_{Ca}1.1$

A) Current density-voltage relationship of whole-cell currents in primary glioblastoma cells. Current densities (J, pA/pF) at the indicated membrane potentials were calculated by dividing the peak current by the cell membrane capacitance. Data were obtained with intracellular solutions containing zero Ca^{2+} (n=11) or 1 µM Ca^{2+} (n=5). **B)** Current density-voltage relationship of whole-cell currents in primary glioblastoma cells (GBM, orange, n=5) and in the U-87 MG glioblastoma cell line (U-87, green, n=5). **C)** Confocal microscopy images of a primary GBM cell. GFAP (top left) was labeled with anti-mouse Alexa 555, the KCa1.1 alpha

subunit was labeled with anti-rabbit Alexa 647, the overlay of the two images is in the top right. The bottom right panel depicts the punctate staining pattern of KCa1.1 with higher magnification. **D)** Representative whole-cell current traces in a primary glioblastoma cell (GBM, left) and in an U-87 cell. Currents were evoked by repeated depolarizations to +100 mV from a holding potential of -100 mV (see voltage pulse on the top) in control extracellular solution (black) and upon reaching equilibrium block in the presence of 1 μM paxilline application (red). **E)** Remaining current fractions ($RCF=I/I_0$ were I_0 and I are the peak currents in the absence and in the presence of the inhibitor, respectively) of the outward currents in primary glioblastoma (GBM) and U-87 cells in the presence of 1 μM paxilline. Black symbols indicate RCF values obtained in individual cells. Throughout the figure data points (or bar heights) are mean ± SEM for the indicated number of experiments.

2.2 K_{Ca}1.1 beta 3 is the main auxiliary subunit associated to the channel in glioblastoma

Auxiliary subunits of K_{Ca}1.1 are known to alter membrane expression of the channel. However, only very limited information is available on β subunit expression in GBM. Thus, we investigated the association of K_{Ca}1.1 to its auxiliary β subunits with both pharmacological methods and genetic modulations.

First, we aimed to determine the functional expression of the β subunits with patch-clamp technique (Fig. 2). Lithocholic acid (LCA) activates K_{Ca}1.1 channels associated with the β1 subunit [21,22], whereas arachidonic acid (AA) activates K_{Ca}1.1 assembled with the β2 or β3 subunits [23]. In primary GBM cells, AA approximately doubles whole-cell K_{Ca}1.1 currents compared to control (Fig. 2B, 1.84-fold increase, p=0.001, two-tailed Wilcoxon test), whereas LCA does not induce K_{Ca}1.1 current increase (Fig. 2A, 1.02-fold increase, p=0.63, two-tailed Wilcoxon test). In contrast, in U-87 MG cells, application of LCA and AA elicit a similar increase in the outward current compared to control (on average 1.38-fold (p=0.0002) and 1.24-fold (p=0.008) current increase, respectively, two-tailed Wilcoxon test, Fig. 2A and 2B). K_{Ca}1.1 channels linked to the β2 subunit have an inactivation time constant around 20 ms [24]. Data in Fig. 2C does not support the involvement of the β2 subunit in regulating the K_{Ca}1.1 currents: whole-cell currents recorded from U-87 MG and primary GBM cells show no inactivation in 100 ms after activation. It also is known that K_{Ca}1.1 channels with β4 subunit are resistant to inhibition by iberiotoxin (IbTx) [25]. However, in both of the primary GBM and U-87 MG cells , 23 nM IbTx (i.e., ~2-10-fold the IC_{50} for K_{Ca}1.1 inhibition [26]), inhibits whole-cell currents (RCF: 0.47 ± 0.04 (n=18) and 0.13 ± 0.03 (n=8) respectively) similarly to 1 μM paxilline (p=0.12 and 0.99 respectively, Student's t tests) (Fig. 2D), thereby ruling out the presence of K_{Ca}1.1 β4 subunits in the channel complex. In summary, the presence of the β1, β2 and β3 subunits in the KCa1.1 complex were favored by the application of

pharmacological modulators of the β subunit-associated channels, while the relevance of the β4 subunit in the cell membrane seems to be highly unlikely with this approach.

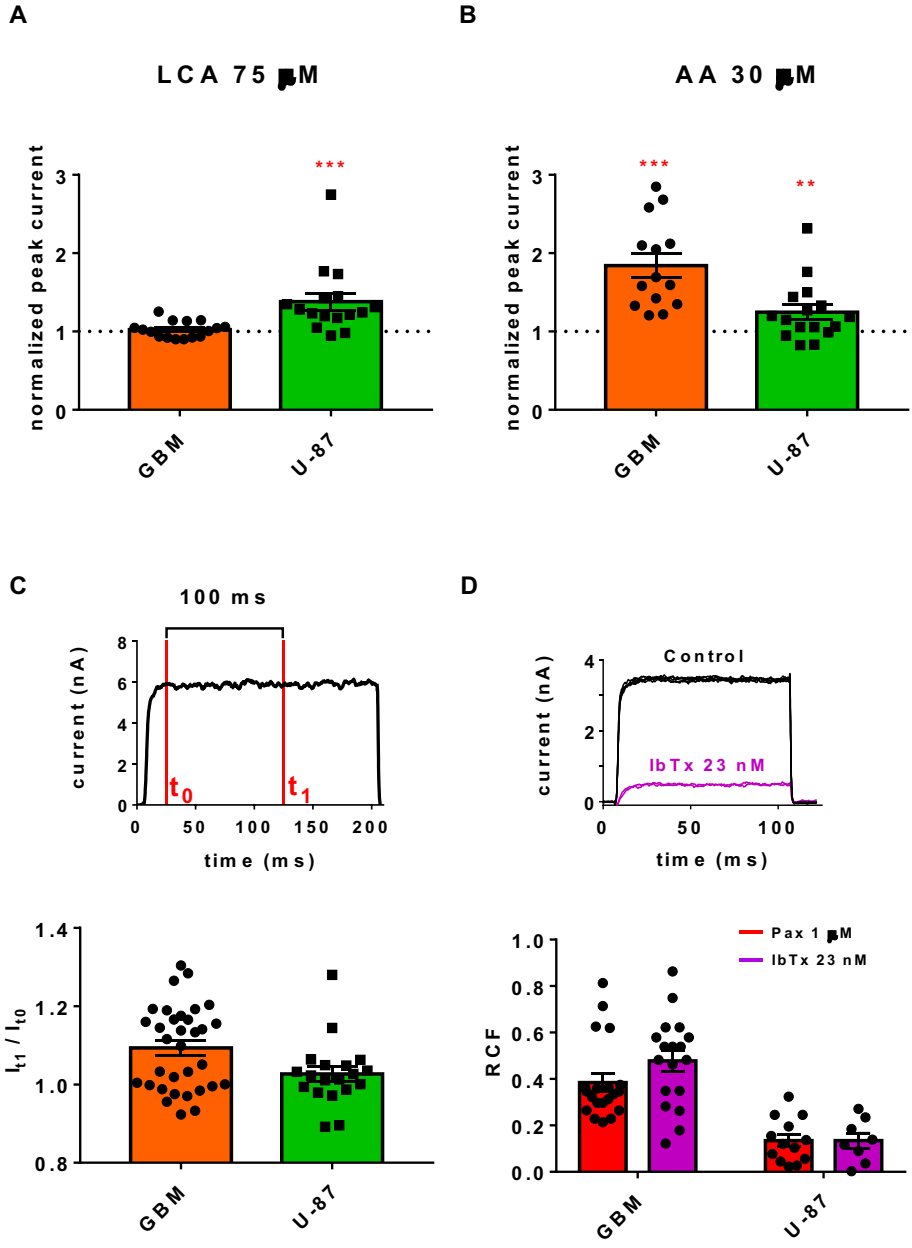

Figure 2. Pharmacological modulators affect β subunit-associated $K_{Ca}1.1$ channels in glioblastoma.

A) The effect of lithocholic acid (LCA, 75 µM) on primary GBM (orange bar, n=16) and U-87 MG cells (green bar, n=16). The current recorded during LCA application was normalized to the current recorded with control solution (dotted line). **B)** The effect of arachidonic acid (AA, 30 µM) on primary GBM (orange bar, n=14) and U-87 MG (green bar n=16) cells. The

current recorded during AA application was normalized to the current recorded with control solution (dotted line). **C)** Channel inactivation in a 100 ms time interval was determined by the current ratio I_{t1}/I_{t0}, where t_0 was the current amplitude at the beginning (20 ms after voltage pulse), and t_1 was the current amplitude at the end of the 100 ms time interval. for primary GBM cells (orange, n=33) and for U-87 cells (green bar, n=19) **D)** The effect of iberiotoxin (IbTx, 23 nM, purple bar, n=8) and paxilline (Pax, 1 μM, red bar, n=13) on the $K_{Ca}1.1$ current in primary GBM and in U-87 cells. Black symbols indicate remaining current fraction (RCF) values obtained in individual cells. RCF is defined in the text and in the legend to Fig. 1. Data represent mean ± SEM, **p<0.01, ***p<0.001

Next, we aimed at supporting the functional data using molecular biology techniques. As indicated in Fig. 3A, several $K_{Ca}1.1$ auxiliary subunit mRNAs are expressed in the U-87 MG cell line. Using RT-qPCR, we found that β1 and β2 subunits are expressed at low levels in both the primary tumor and U-87 MG cells, whereas the β3 subunit shows the highest expression (Supp. Fig. 1 for primary GBM). Using Western blot, we validated that $K_{Ca}1.1$ β2 and β3 subunit proteins are expressed in U-87 MG cells, whereas the $K_{Ca}1.1$ β1 band is absent (Fig. 3B).

As small-molecule pharmacological modulators such as lithocholic acid and arachidonic acid are quite promiscuous and activate multiple other ion channels and signaling pathways [27,28], we applied genetic modulation of U-87 MG cells using siRNA targeting different $K_{Ca}1.1$ β subunits. We validated the silencing using Western Blot 48 h following application of siRNA (Fig. 3B). In these experiments Chinese hamster ovary (CHO) cells were used as positive control for β1 (KCNMB1) and β3 (KCNMB3) expression [29]. Non-silenced U-87 cells express both $K_{Ca}1.1$ β2 (KCNMB2) and β3 (KCNMB3) proteins, which cannot be detected upon silencing the corresponding β subunit. As demonstrated in Fig 3C, lithocholic acid has a similar effect on whole-cell currents after $K_{Ca}1.1$ β1 silencing compared to the scrambled siRNA control (p=0.63, unpaired, two-tailed t-test, $N_{silence}$=3). In contrast, both $K_{Ca}1.1$ β2 and β3 siRNA decrease the response of U-87 MG cell to arachidonic acid compared to scrambled RNA silencing (p=0.083 and p=0.038, respectively) (Fig. 3D and 3E). Taken together the higher sensitivity of the β3 silencing on the AA response (Fig. 3E) and the larger expression of the β3 RNA compared to other auxiliary subunits (Fig. 3A) we propose that $K_{Ca}1.1$ β3 is the main auxiliary subunit associated to $K_{Ca}1.1$ in the membrane of glioblastoma cells.

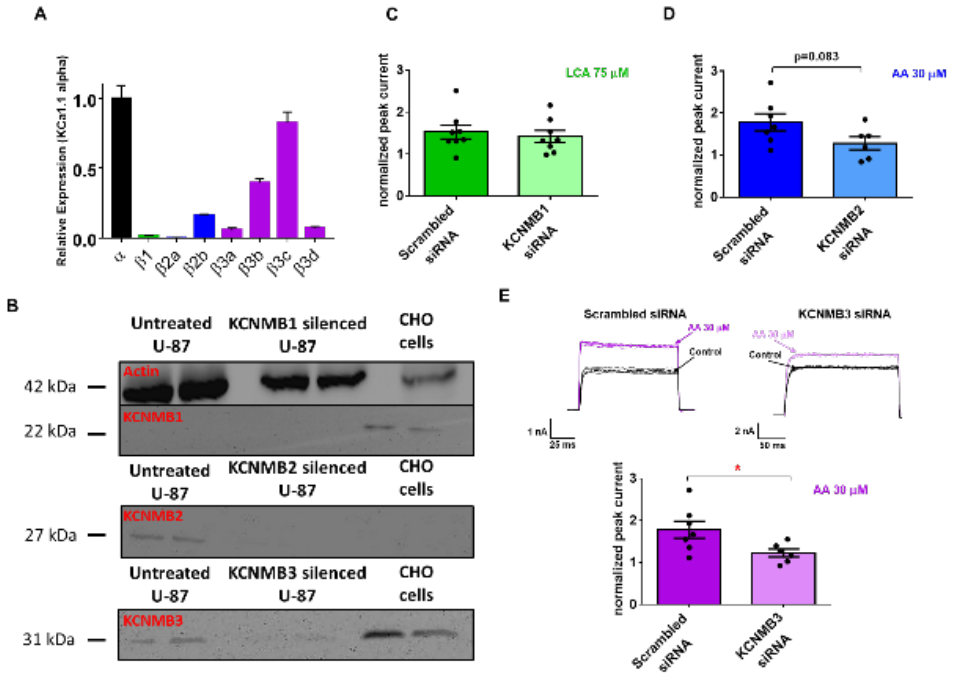

Figure 3. Gene silencing confirms dominant KCa1.1 β 3 subunit expression.

A) Results of qPCR experiments assessing the relative expression of the beta subunits (black bar) in the U-87 MG cell line. β1, β2 and β3 mRNA levels divided by the expression of the K_{Ca}1.1 channel α-subunit are represented with green, blue and purple bars respectively (N=3, n=3). **B)** Western blot of the untreated and gene silenced U-87 cells. The populations were tested in duplicate, the left two lanes are the untreated U-87 cells and the right two lanes are CHO cells. The middle lane pairs are for the KCNMB1, KCNMB2 and KCNMB3 silenced populations, from top to bottom, respectively. The thick band in the top box at 42 kDa corresponds to actin and the 22 kDa marker to KCNMB1. In the second box (middle) the KCNMB2 bands are shown (27 kDa marker), and in the third box (bottom) the KCNMB3 band are shown (31 kDa marker). (C to E) Pharmacological studies after gene silencing ($N_{Silence}$=3). Whole-cell currents were recorded as in Fig1D, peak currents were measured and normalized peak current was calculated as in Fig 2A and B. **C)** Effect of 75 µM LCA on control scrambled siRNA (dark green bar, n=8) and on KCNMB1 siRNA transfected (light green bar, n=8) U-87 MG cells. **D)** Effect of 30 µM AA on the KCNMB2 (light blue bar, n=6), and **E)** on the KCNMB3 siRNA treated cells (light purple bar, n=6), compared to the scrambled siRNA transfected groups (dark blue and dark purple bars respectively, n=7). Insets in E show the raw currents obtained in a scrambled RNA (left) and in a KCNMB3 siRNA treated cell before (Control) and after the application of 30 um AA. Voltage protocols are in Fig.1D. Throughout the figure, bar heights are mean ± SEM for the indicated number of experiments, *p<0.05.

2.3 $K_{Ca}1.1$ β3 is involved in U-87 MG Ca^{2+} signaling but shows no cell cycle dependence

To investigate whether the $K_{Ca}1.1$ β3 subunit is involved in downstream mechanisms of $K_{Ca}1.1$ function, we studied the intracellular Ca^{2+} signaling evoked by the acetylcholine (Ach) analogue, carbachol [14,30](Fig. 4). Fig. 4A left panel shows that U-87 MG cells respond to the application of 10 μM carbachol (combined with the solvent for paxillin, DMSO) with a marked increase in the cytosolic free Ca^{2+} concentration, as reported by the increased F_{340}/F_{380} ratio. The Ca^{2+}- response of the cells is inhibited by the simultaneous administration of carbachol and 1 μM paxilline (Fig. 4A, right panel). The heat maps in Fig. 4B highlight that approximately half of the cells in each population (59 of 120 cells in the control group, 49 of 91 cells in the carbachol + paxilline-treated group) respond to cholinergic stimulation by a more than 20% increase in the F_{340}/F_{380} ratio compared to their initial value. The statistical analysis (Fig. 4C) clearly indicates that paxilline (n=49 cells; peak F_{340}/F_{380}= 1.6 ± 0.06) inhibits the Ca^{2+}- response of the U-87 MG cells to carbachol (n= 59 cells; peak F_{340}/F_{380}= 2.1 ± 0.07; $p<0.0001$). Interestingly, the peak of the carbachol-induced Ca^{2+} signal (Fig. 4D) at t = 220s is inhibited by KCNMB3 silencing (n=30; p=0.0004) similarly to silencing of the pore forming subunit of $K_{Ca}1.1$ (n=51; p=0.025). The F_{340}/F_{380}, ratios at t = 220s were 1.1 ± 0.06 (n=39) for the siGAPDH treatment, 0.8 ± 0.04 (n=51) for the siKCNMA1 (siKCNMA1) and 0.9 ± 0.04 for siKCNMB3 treatments (n=30), (Fig 4D). Based on these data we conclude that $K_{Ca}1.1$ coupled to the β3 subunit mediates Ca^{2+}-signaling in response to carbachol in U-87 MG cells.

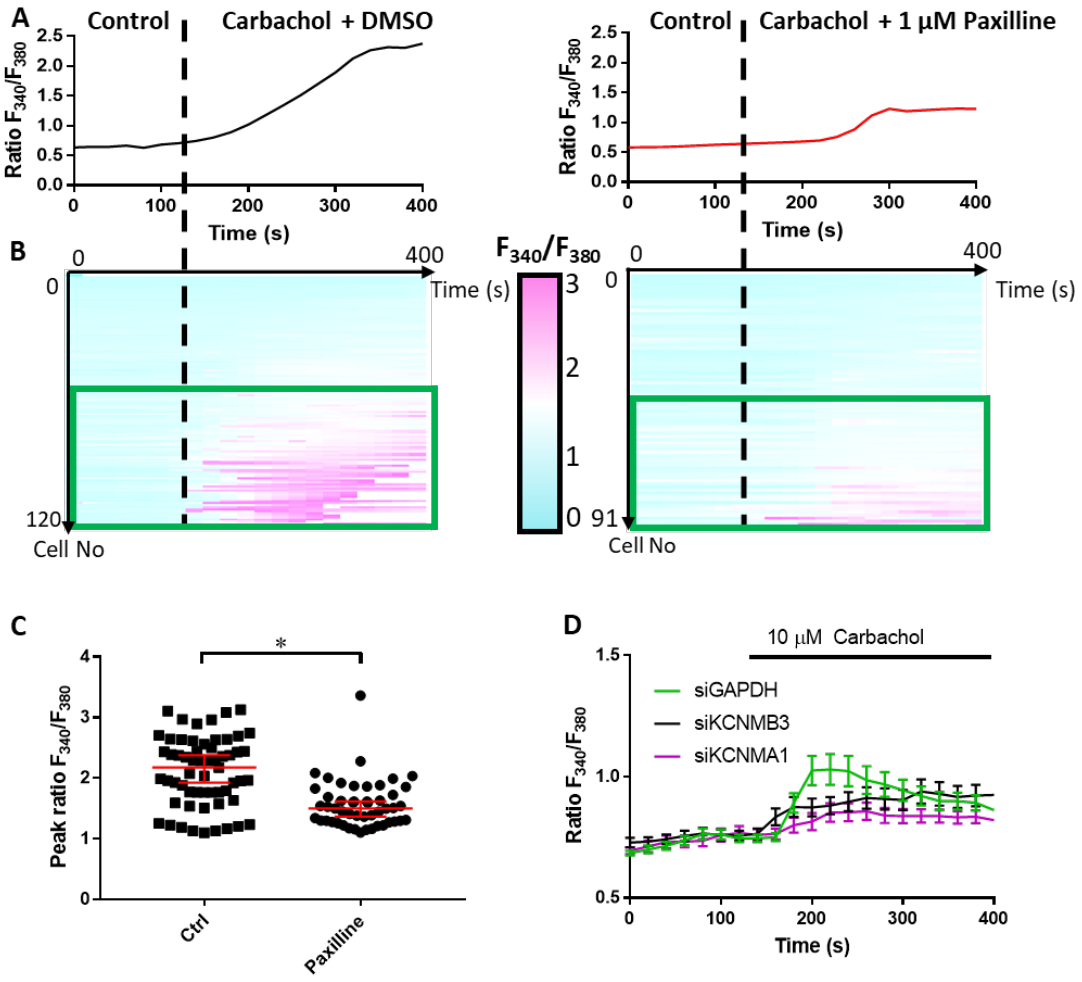

365 Figure 4. K_{Ca}1.1 beta 3 is involved in the $Ca2^{+}$-response of U87-MG cells

366 **A)** Representative intracellular Ca^{2+} measurements, where F_{340}/F_{380} ratio is directly
367 proportional to the intracellular Ca^{2+} concentration. Dotted line shows start of carbachol.
368 superfusion after 2 min superfusion with control [(left panel: black line, 0.1% DMSO in 10
369 µM carbachol-containing solution, N=5, n=120); or in combination with paxilline (right panel:
370 red line, 10 µM carbachol + 1 µM paxilline, (N=5, n=91). **B)** Heat map depicting the F_{340}/F_{380}
371 ratio response over time (x axis) for each individual cell measured (y axis). Pseudocolor code
372 shows increasing Ca^{2+} concentrations with more magenta-toned color. Green rectangle
373 confines cells showing >20% increase in F_{340}/F_{380} ratio after carbachol superfusion. **C)** Peak
374 of the 10 µM carbachol-induced F_{340}/F_{380} ratio (see A and B for details) of control superfused
375 cells (n=59, N=3) and 1 µM paxilline-treated cells (n=49, N=3). **D)** Carbachol-elicited
376 intracellular Ca^{2+} response of cells after silencing of GAPDH (green, siGAPDH, N=3, n=39
377 (F_{340}/F_{380}= 1.1 ± 0.06), K_{Ca}1.1 (purple, siKCNMA1, N=3, n=51 (F_{340}/F_{380}= 0.8 ± 0.04) and
378 K_{Ca}1.1 beta 3 (black, siKCNMB3, N=3, n=30 (F_{340}/F_{380}= 0.9 ± 0.04)). In C) and D) data are
379 mean ± SEM for the indicated number of experiments, *p<0.05.

As cytosolic Ca^{2+} fluctuates during the cell cycle, and K^+ channels are expressed in a cell cycle-dependent manner [31,32], we aimed at testing whether the $K_{Ca}1.1$ β3 subunit regulates the cell cycle of glioblastoma cells. To this end, we synchronized U-87 MG cells in M phase using colchicine and in G_0 phase using serum starvation (Fig. 5.). Fig. 5A shows the flow cytometry data of the synchronized cells. The histograms and Suppl. table 1 show that 36 ± 3 % of the cells were in G_2/M phase 24 h following 10 µM colchicine treatment (N=3, n=3) as compared to 16 ± 1% in the untreated group (N=3, n=5). Upon serum starvation, a high percentage of cells reside in the G_0/G_1 phase (57 ± 3% for untreated, 78 ± 1% for serum starvation, N=3, n=5 and N=2, n=2, respectively) (Supp. Table 1.). Interestingly, we observed a marked increase in the magnitude of the whole-cell currents in M phase synchronized cells as compared to control (non-synchronized, untreated) and G_0 synchronized ones (Fig. 5B-C). The increase in the peak currents become evident at depolarizations to +40 mV or above (Mann-Whitney test, Fig. 5C). As cell volume and cell surface are can also change during the cell cycle [33], we also determined current density (J, see above). Similar to the peak currents, the current density was significantly larger in the M phase synchronized cells as compared to control and G_0 phase synchronized ones at depolarized test potentials (above +20 mV, Mann-Whitney test, Fig. 5D). To ensure that the main component of the whole-cell currents is still $K_{Ca}1.1$, we applied paxilline (1 µM) to each synchronized and control cell population (Fig. 5E). We found a pronounced inhibition of the whole cell K^+ current by paxilline in all cell cycle phases, especially in the M phase, the average RCF in colchicine- and serum starvation-treated cells were 0.05 ± 0.01 (n=9) and 0.17 ± 0.02 (n=10), respectively (p=0.007, Kruskal-Wallis test, Fig. 5E). This confirms that the major current component is $K_{Ca}1.1$ in colchicine-synchronized cells. On the other hand, the increase in the whole-cell current induced by 30 µM AA was similar in all groups (current increase: 1.26 ± 0.09 (n=16), 1.1 ± 0.08 (n=10) and 1.09 ± 0.03 (n=10) for the untreated, colchicine- and serum starvation treated cells respectively, p=0.46, Kruskal-Wallis test, Fig. 5F). Together, these results indicate that $K_{Ca}1.1$ function is increased after M phase synchronization, without alterations in the β3 subunit-dependent modulation in the K^+ current.

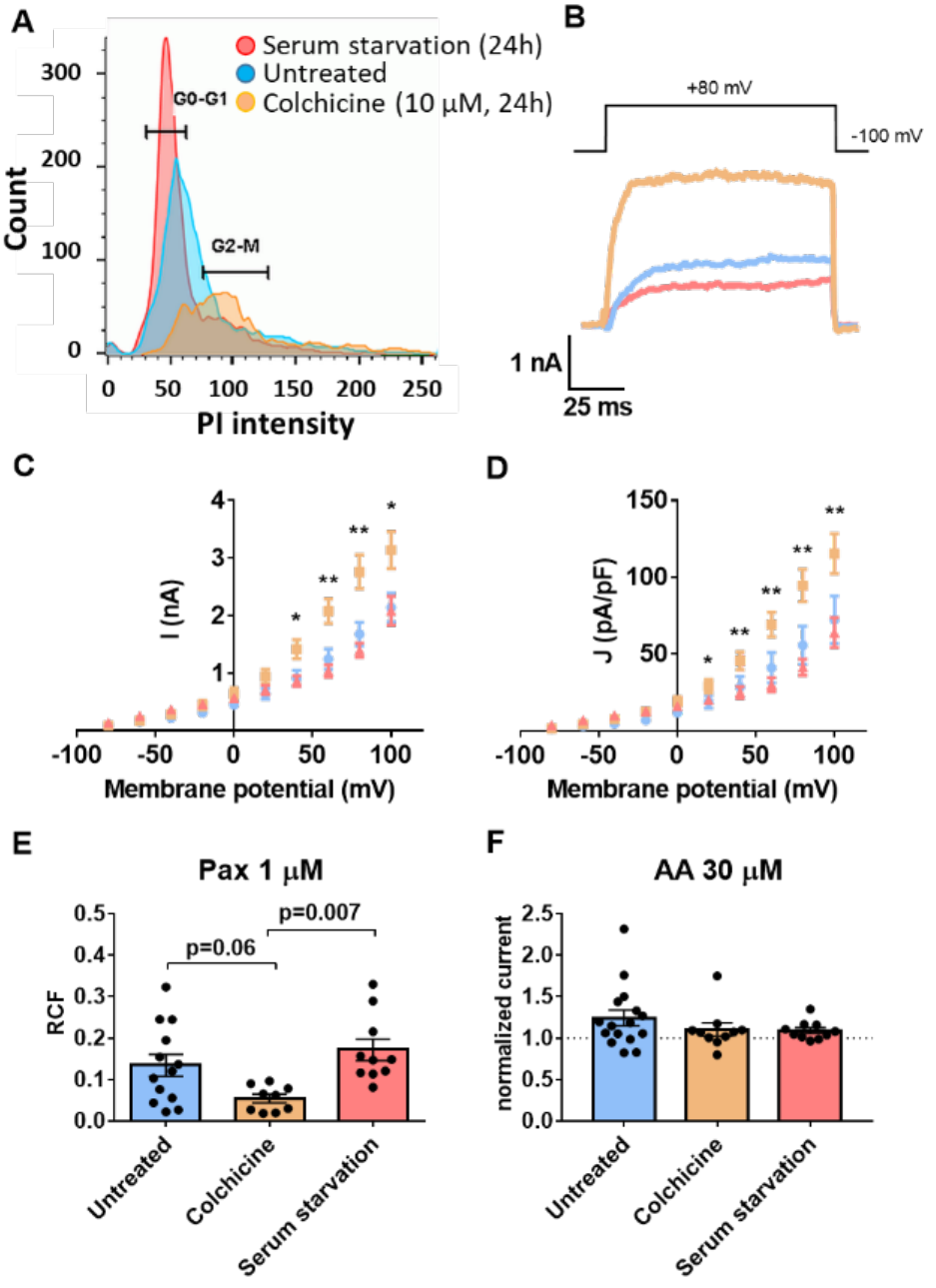

Figure 5. $K_{Ca}1.1$, but not the beta 3 subunit shows cell cycle-dependent function

A) Flow cytometry of colchicine treated (4 µg/ml, 24h; in orange), starving (serum free DMEM, 24h; in red) and untreated U-87 MG cells (in blue), where propidium iodide (PI) intensity is shown as a function of cell count. **B)** Representative patch-clamp traces of the serum starved (red), colchicine-treated (orange) and untreated (blue) populations, respectively. The displayed currents were recorded at +80 mV depolarizing pulse with 4 µM free Ca^{2+} in

the pipette-filling solution. **C)** Current amplitude (I, nA) as a function of membrane potential (mV) for control (untreated, blue, n=20), for colchicine-treated (orange n=19), and starving cells (n=9). Whole-cell currents were obtained as in Fig 1A, 4μM free Ca^{2+} in the pipette-filling solution). **D)** Current density (J, pA/pF) as a function of membrane potential (mV) was calculated for n=18 control (blue), n=18 colchicine-treated (orange) and n=7 starving cells(red) from the data in panel C. In panels C and D the star symbols indicate the significant difference between the colchicine treated and the untreated cells. **E)** Effect of 1 μM paxilline on the whole cell currents in untreated (n=13), colchicine-treated (n=9) and starving cells (n=10). Black symbols indicate RCF values obtained in individual cells, RCF was calculated as in Fig 1) **F)** The effect of 30 μM AA on the normalized current in untreated (n=16), colchicine-treated (n=10) and starving cells (n=10). Bars indicate the current amplitude measured with AA superfusion normalized to the current amplitude measured with control solution. Throughout the figure data points (or bar heights) are mean ± SEM for the indicated number of experiments, *: $p<0.05$; **: $p<0.01$.

2.4 $K_{Ca}1.1$ inhibition has an additive effect with temozolomide on U-87 MG viability

Alkylating agents, such as temozolomide affect the cell cycle of glioblastoma cells by synchronizing them in the G_2 phase [34]. In the previous section we described that colchicine-synchronized U-87 MG have increased $K_{Ca}1.1$ current density (Fig. XX). Thus, we wanted to exploit this phenotype by testing whether $K_{Ca}1.1$ inhibition potentiates temozolomide chemotherapy. We investigated the short-term effects of TMZ and the $K_{Ca}1.1$ inhibitor separately or in combination over the first few hours of treatment with time-lapse video microscopy (Suppl. Video 1), where we evaluated the migration of U-87 MG cells. As shown in Fig. 6A and 6B, we found that TMZ (500 μM) alone does not inhibit the velocity of two-dimensional spontaneous cell migration over 6 h as compared to control (0.53 ± 0.04 μm/min, N=3, n=28 vs. 0.53 ± 0.03 μm/min, N=3, n=30, $p>0.99$). In contrast, paxilline alone and in combination with temozolomide inhibit cell migration velocity similarly, by ≈ 50% (0.2 ± 0.03 μm/min, N=3, n=30 and 0.3 ± 0.03 μm/min, N=3, n=30, respectively).

As U-87 MG cells appear viable at the end of the 6h time-lapse of the paxillin + temozolomide treatment, we hypothesized that longer treatment time would be necessary for the alkylating agent to take effect. Therefore, we tested the effects of paxilline and TMZ on cell viability 48h after treatment (Fig. 6C and 6D). Here, compared to control treatment (normalized cell survival, a.u.: 1±0.02, N=4, n=32), we found a slight inhibition of cell

viability when applying paxilline alone (0.84 ± 0.03, N=4, n=16, p<0.0001) or temozolomide alone (0.77 ± 0.03, N=4, n=15, p<0.0001). The latter effect of temozolomide was potentiated by applying the two compounds in combination (0.63 ± 0.03, N=4, n=15, p<0.0001). Based on these results we concluded that paxilline has an additive effect to temozolomide on the viability of U-87 MG cells, which evolves over the course of days rather than hours.

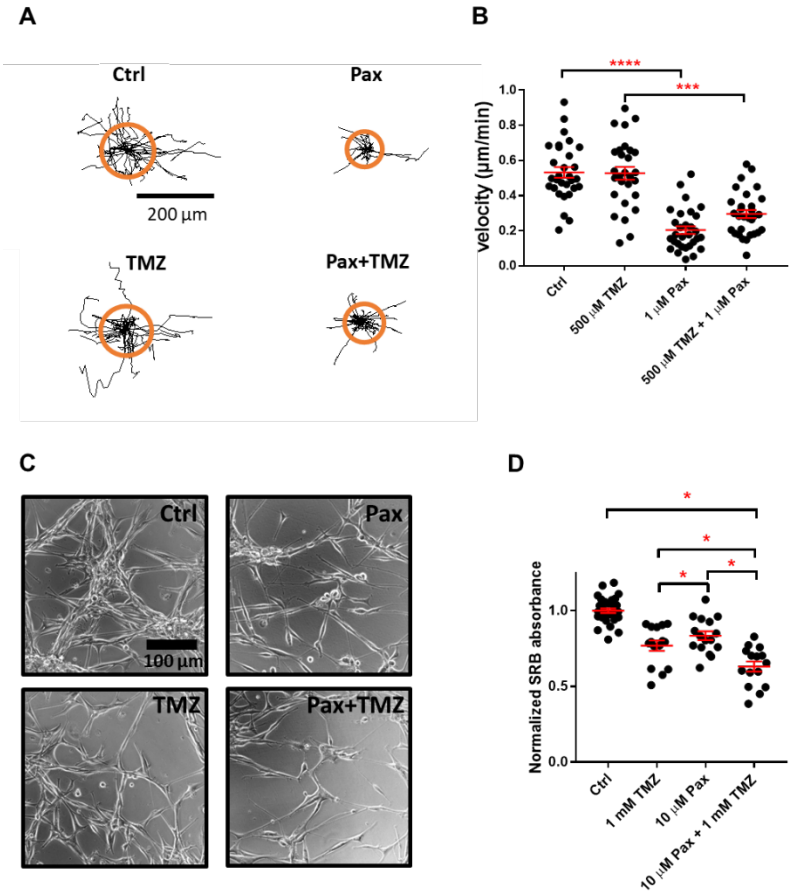

Figure 6. Additive effects of paxilline and temozolomide on cell viability

A) Migration trajectories of U-87 MG cells (black lines) over 6h treated with 0.1% DMSO (Ctrl), 500 µM temozolomide (TMZ), 10 µM paxilline (Pax) and combined 10 µM paxilline + 500 µM temozolomide (Pax+TMZ) treatment. Orange circle indicates the mean start-to-end translocation. **B)** Scatter plot shows quantification of migration velocities (µm/min) of U-87 MG cells depicted in panel (A) (N=3, n=30). **C)** Representative phase-contrast microscopy images of U-87 MG cells treated for 48h with 10 µM Pax and/or 1 mM TMZ, as indicated on the panels **D)** Cell viability was determined by sulforhodamine B (SRB) assay after 48 h by normalizing the SRB absorbance in the treatment group to the SRB absorbance upon control

(Ctrl) treatment (N=4, n=32) after 48 h paxilline and/or temozolomide (N=4, n=15) treatment, *p< 0.05, ***p<0.001, ****p<0.0001

3 Discussion

In this study, we showed that the Ca^{2+}-dependent K^+ channel $K_{Ca}1.1$ functions in the plasma membrane of patient-derived primary glioblastoma cells as well as the U-87 MG cell line in association with its auxiliary β3 subunit (Fig. 1, 2 and 3), which has a consequence on cellular Ca^{2+} signaling (Fig. 4) but not on cell cycle progression (Fig. 5). The main relevance of this finding is that even though $K_{Ca}1.1$ is ubiquitously expressed in many tissues in the human body, ancillary beta subunits have a much more restricted tissue expression. Particularly, the β3 subunit is rarely found in healthy tissues [35], and has only been described to date in the testes, pancreas and spleen. This, and its membrane localization makes the β3 subunit an attractive target for glioblastoma diagnosis and/or therapy, specially knowing that the increased expression of $K_{Ca}1.1$ β3-encoding gene KCNMB3 correlates with poor survival of GBM patients [9]. Therefore, synthetizing auxiliary subunit binding specific probes are warranted in a future study.

To our knowledge, we are the first to describe that $K_{Ca}1.1$, coupled to the auxiliary β3 subunit, provides the driving force for Ca^{2+} influx after Ach receptor stimulation (Fig. 4). Generally, the function of ancillary ion channel subunits is to fine-tune the expression and biophysical properties of the pore-forming (here $K_{Ca}1.1$ α) subunit [8,36,37]. It has been recently proposed that Ach-dependent signals, in a Ca^{2+}-dependent manner, induce matrix metalloprotease 9, which ultimately increases glioblastoma cell invasiveness [15]. In contrast, overall cell migration is inhibited by carbachol application (Supp. Fig. 2), which is confirmed by previous evidence [14].

In addition, this study provides the first description that the chemotherapeutic agent temozolomide has an additive effect with $K_{Ca}1.1$ inhibition on U-87 MG cell viability (Fig. 6). Our results align well with another recent finding that blocking $K_{Ca}1.1$ inhibits hypoxia-induced chemoresistance of GBM cells against cisplatin [7]. Earlier, it has also been shown that TMZ treatment upregulates the gBK isoform of $K_{Ca}1.1$, possibly thereby enhancing therapeutic effects [38]. Here, we propose an additional mechanism for the long-term inhibition of cell viability: $K_{Ca}1.1$ currents are enhanced in colchicine-treated, metaphase synchronized U-87 MG cells (Fig. 5), supporting that K^+ channels have an important role in the cell division machinery [31]. Previously, it has been shown that $K_{Ca}1.1$ is involved in the radiosensitivity in GBM: tumor cells that have been previously irradiated by 2 Gray have more prominent $K_{Ca}1.1$ function than control cells [6]. Also, when treating orthotopic glioblastoma tumors of mice with a combination of radiotherapy and paxilline, tumors were markedly reduced compared to controls. Moreover, similarly to $K_{Ca}1.1$, it is known that the Ca^{2+}-activated, but voltage-insensitive $K_{Ca}3.1$ channel sensitizes GBM cells to TMZ therapy [39]. Based on our results we propose that $K_{Ca}1.1$

inhibition in GBM may not only be co-applied with radiotherapy but could also be utilized together with chemotherapy. This is especially important as most patients having GBM undergo a complex treatment plan involving both chemo-and radiotherapy as well as surgery.

Interestingly, in disease, the $K_{Ca}1.1$ channel together with the β3 subunit is also functional in fibroblast-like synoviocytes in rheumatoid arthritis [40]. One explanation for this can be that both glioblastoma and rheumatoid arthritis are accompanied by pronounced inflammation altering multiple parameters such as pH and the mechanical environment [41–43]. For example, it has been described that the mechanosensitivity of $K_{Ca}1.1$ conferred by the auxiliary β1 subunit in vascular smooth muscle [44]. Whether alterations in the microenvironment indeed modify auxiliary subunit expression via a common mechanism in diseases involving inflammation, however, remains to be tested.

We also investigated whether other auxiliary subunits are associated with $K_{Ca}1.1$ in the membrane of glioblastoma cells (Fig. 2 and 3). The β1 subunit, prominently expressed in smooth muscle cells, prolongs activation kinetics of $K_{Ca}1.1$ and has a well characterized pharmacological activation by bile acids [8,21,45,46]. Even though ionic currents of primary GBM and U-87 MG cells are activated by 75 µM lithocholic acid, two factors argue against the presence of $K_{Ca}1.1$ β1 in glioblastoma cells. First, we could not detect $K_{Ca}1.1$ β1 in RT-qPCR (Fig. 4A) and Western Blot (Fig. 4B). Also, in response to LCA we observed similar pharmacological response in KCNMB1-silenced cells as in the scrambled siRNA-treated controls. Knowing that bile acids activate a multitude of other ion channels, e.g. bile acid sensitive ion channels (BASIC) [47], it is much more likely that LCA acts on different ion channels than $K_{Ca}1.1$ in glioblastoma cells. Regarding the β2 subunit of $K_{Ca}1.1$, we found that it is present in the cells as mRNA and protein also, using RT-qPCR and Western Blot, respectively. β2 subunits are similar to β3 subunits in a manner that arachidonic acid activates the $K_{Ca}1.1$. channels associated to them [23,28]. Also, KCNMB2-silenced U-87 MG cells show less AA-dependent response compared to control-silenced cells, indicating its presence in the cell membrane. However, β2 subunits lead to a rapid inactivation of $K_{Ca}1.1$-mediated currents, which we only rarely (n=2 out of n=51 primary GBM cells) observed in our setting, with most whole-cell currents showing no inactivation over 200 ms (Fig. 2C). Why channel inactivation was absent can be explained by a change in stoichiometry between the different β subunits associated to $K_{Ca}1.1$ α: as four possible β subunits can simultaneously bind to one functional channel [48], the ratio of different β subunits associated with the channel may become very important, as indicated previously [49,50]. In GBM, a biological consequence of altered subunit stoichiometry is easily possible: more β2 subunits linked to one $K_{Ca}1.1$ channel

would mean faster inactivation, thus less Ca^{2+} signals, whereas more β3 subunits would lead to an absence in channel inactivation and a prolonged Ca^{2+} influx. Therefore, thorough assessment is warranted in a further study to prove this concept in GBM. The $K_{Ca}1.1$ β4 subunit is known to be expressed in the central nervous system [35,51]. In transfected model cells, $K_{Ca}1.1$ channels coupled to β4 subunit become resistant to inhibition by the peptide toxin IbTx [25,52]. In contrast, we observed that iberiotoxin inhibits whole-cell currents potently (Fig. 2D). Thus, it is likely that the beta 4 subunit is not associated with $K_{Ca}1.1$ in glioblastoma. Lastly, $K_{Ca}1.1$ gamma subunits, are unlikely in GBM cells: as $K_{Ca}1.1$ channels associated with γ subunits already open at very negative membrane potentials of –150 mV [53]. In comparison, $K_{Ca}1.1$ starts to open at much less negative membrane potential in primary GBM as well as in U-87 MG cells (Figure 1A). In summary, besides the evident association of $K_{Ca}1.1$ channels to β3 in the plasma membrane of GBM cells, it is likely that a minority of the channels are be coupled to β2.

4 Conclusion

To summarize, we found that $K_{Ca}1.1$ channels are coupled primarily to the auxiliary β3 subunit on the cell membrane of glioblastoma and U-87 MG cells, whereas the β2 subunit only show a minor involvement in the channel phenotype in these cells. The β3-associated $K_{Ca}1.1$ channels are involved in Ca^{2+}-signaling of GBM cells after muscarinic acethycholine receptor activation. Importantly, $K_{Ca}1.1$ becomes up-regulated in the G_2/M phase of the cell cycle by a beta-subunit independent manner that remains to be elucidated. By inhibiting $K_{Ca}1.1$ with the small molecule inhibitor paxilline, U-87 MG cell viability decreases, which is also potentiated by the co-application with the chemotherapeutic drug temozolomide. This aligns well with the literature, as the temozolomide causes an arrest in the G_2/M phase, where we saw the above mentioned dominancy of the channel [34]. In conclusion, we propose the $K_{Ca}1.1$ channel as a supportive drug target in GBM chemotherapy and the β3 subunit as a membrane-localized marker for glioblastoma cells to be exploited for diagnostic or therapeutic approaches.

5 Author contributions

Z.P. and G.P. conceived the study, which was developed together with A.F. and Z.V.. A.K. obtained glioblastoma patient samples, and T.H. performed histopathological analysis. T.G.Sz., G.T., A.F. and Z.P. performed patch clamp measurements. Synchronization and cell cycle measurements were done by G.B., G.T. and A.F. Intracellular Ca^{2+} measurements, cell migration and viability studies were performed by Z.P. in discussion with A.S. The manuscript and figures were prepared by A.F. and Z.P. All authors read and approved the manuscript.

6 Acknowledgements

We would like to thank Cecilia Nagy and Adrienn Bagosi for their excellent technical support. The study was funded by NKFIH K119417 to GP . Z.P. was supported by the ÚNKP-16-3-I. A.K. was supported by the 2017-1.2.1-NKP-2017-00002 "National Brain Research Program NAP 2.0".

7 Data availability

The data that supports the findings is available upon request from the corresponding author panyi@med.unideb.hu

8 Conflict of interests

The authors declare no conflict of interest.

9 Figures and Figure Legends

9.1 Figure 1.

Placeholder until the end

10 References

1 Tan AC, Ashley DM, López GY, Malinzak M, Friedman HS & Khasraw M (2020) Management of glioblastoma: State of the art and future directions. *CA Cancer J Clin* **70**, 299–312.

2 V H, K N, M R, R B, M C, A A, G P, A S, Hofschröer V, Najder K, Rugi M, Bouazzi R, Cozzolino M, Arcangeli A, Panyi G & Schwab A (2021) *Ion Channels Orchestrate Pancreatic Ductal Adenocarcinoma Progression and Therapy*.

3 Capatina AL, Lagos D & Brackenbury WJ (2020) Targeting Ion Channels for Cancer Treatment: Current Progress and Future Challenges. , 1–43.

4 Liu X, Chang Y, Reinhart PH & Sontheimer H (2002) Cloning and characterization of glioma BK, a novel BK channel isoform highly expressed in human glioma cells. *J Neurosci* **22**, 1840–1849.

5 Ransom CB, Liu X & Sontheimer H (2002) BK channels in human glioma cells have enhanced calcium sensitivity. *Glia* **38**, 281–291.

6 Edalat L, Stegen B, Klumpp L, Haehl E, Schilbach K, Lukowski R, Kühnle M, Bernhardt G, Buschauer A, Zips D, Ruth P & Huber SM (2016) BK K+ channel blockade inhibits radiation-induced migration/brain infiltration of glioblastoma cells. *Oncotarget* **7**, 14259–14278.

7 Rosa P, Catacuzzeno L, Sforna L, Mangino G, Carlomagno S, Mincione G, Petrozza V, Ragona G, Franciolini F & Calogero A (2018) BK channels blockage inhibits hypoxia-induced migration and chemoresistance to cisplatin in human glioblastoma cells. *J Cell Physiol* **233**, 6866–6877.

8 Li Q & Yan J (2016) Modulation of BK Channel Function by Auxiliary Beta and Gamma Subunits. *Int Rev Neurobiol* **128**, 51–90.

9 Ge L, Hoa NT, Wilson Z, Arismendi-Morillo G, Kong XT, Tajhya RB, Beeton C & Jadus MR (2014) Big Potassium (BK) ion channels in biology, disease and possible targets for cancer immunotherapy. *Int Immunopharmacol* **22**, 427–443.

10 Turner KL, Honasoge A, Robert SM, Mcferrin MM & Sontheimer H (2014) A proinvasive role for the Ca(2+) -activated K(+) channel KCa3.1 in malignant glioma. *Glia* **62**, 971–981.

11 Souza DG, Bellaver B, Souza DO & Quincozes-Santos A (2013) Characterization of adult rat astrocyte cultures. *PLoS One* **8**.

525 12 Kuntze A, Goetsch O, Fels B, Najder K, Unger A, Wilhelmi M, Sargin S,
526 Schimmelpfennig S, Neumann I, Schwab A & Pethő Z (2020) Protonation of Piezo1
527 Impairs Cell-Matrix Interactions of Pancreatic Stellate Cells. *Front Physiol* **11**.

528 13 Waschk DEJ, Fabian A, Budde T & Schwab A (2011) Dual-color quantum dot
529 detection of a heterotetrameric potassium channel (hKCa3.1). *Am J Physiol Cell*
530 *Physiol* **300**.

531 14 Bordey A, Sontheimer H & Trouslard J (2000) Muscarinic activation of BK channels
532 induces membrane oscillations in glioma cells and leads to inhibition of cell
533 migration. *J Membr Biol* **176**, 31–40.

534 15 Thompson EG & Sontheimer H (2019) Acetylcholine Receptor Activation as a
535 Modulator of Glioblastoma Invasion. *Cells* **8**.

536 16 R Core Team (2021) R: A language and environment for statistical computing. .

537 17 Dieterich P, Klages R, Preuss R & Schwab A (2008) Anomalous dynamics of cell
538 migration. *Proc Natl Acad Sci U S A* **105**, 459–463.

539 18 Vichai V & Kirtikara K (2006) Sulforhodamine B colorimetric assay for cytotoxicity
540 screening. *Nat Protoc* **1**, 1112–1116.

541 19 Cox DH (2014) Modeling a Ca2+ channel/BKCa channel complex at the single-
542 complex level. *Biophys J* **107**, 2797–2814.

543 20 Kraft R, Krause P, Jung S, Basrai D, Liebmann L, Bolz J & Patt S (2003) BK channel
544 openers inhibit migration of human glioma cells. *Pflugers Arch* **446**, 248–255.

545 21 Dopico AM, Walsh J V. & Singer JJ (2002) Natural Bile Acids and Synthetic
546 Analogues Modulate Large Conductance Ca2+-activated K+ (BKCa) Channel
547 Activity in Smooth Muscle Cells. *J Gen Physiol* **119**, 251.

548 22 Bukiya AN, Vaithianathan T, Toro L & Dopico AM (2009) Channel beta2-4 subunits
549 fail to substitute for beta1 in sensitizing BK channels to lithocholate. *Biochem*
550 *Biophys Res Commun* **390**, 995–1000.

551 23 Sun X, Zhou D, Zhang P, Moczydlowski EG & Haddad GG (2007) Beta-subunit-
552 dependent modulation of hSlo BK current by arachidonic acid. *J Neurophysiol* **97**,
553 62–69.

554 24 Xia XM, Ding JP & Lingle CJ (2003) Inactivation of BK channels by the NH2 terminus
555 of the beta2 auxiliary subunit: an essential role of a terminal peptide segment of three
556 hydrophobic residues. *J Gen Physiol* **121**, 125–148.

557 25 Meera P, Wallner M & Toro L (2000) A neuronal beta subunit (KCNMB4) makes the
558 large conductance, voltage- and Ca2+-activated K+ channel resistant to
559 charybdotoxin and iberiotoxin. *Proc Natl Acad Sci U S A* **97**, 5562–5567.

560 26 Tanner MR, Pennington MW, Chamberlain BH, Huq R, Gehrmann EJ, Laragione T,
561 Gulko PS & Beeton C (2018) Targeting KCa1.1 Channels with a Scorpion Venom
562 Peptide for the Therapy of Rat Models of Rheumatoid Arthritis. *J Pharmacol Exp*
563 *Ther* **365**, 227.

564 27 Kiriyama Y & Nochi H (2019) The Biosynthesis, Signaling, and Neurological
565 Functions of Bile Acids. *Biomol 2019, Vol 9, Page 232* **9**, 232.

566 28 Antollini SS & Barrantes FJ (2016) Fatty Acid Regulation of Voltage- and Ligand-
567 Gated Ion Channel Function. *Front Physiol* **7**.

568 29 Garza Lopez E, Sánchez-Carranza O, Nishigaki T & López-González I (2015)
569 Pharmacological identification of endogenous Slo1 channel-B1 subunit complexes in
570 CHO cells using three aKTX1 subfamily toxins. *Int J Pharm Ther* **6**, 11–24.

571 30 Thompson EG & Sontheimer H (2019) Acetylcholine Receptor Activation as a
572 Modulator of Glioblastoma Invasion. *Cells* **8**.

573 31 Urrego D, Tomczak AP, Zahed F, Stühmer W & Pardo LA (2014) Potassium channels
574 in cell cycle and cell proliferation. *Philos Trans R Soc B Biol Sci* **369**.

575 32 Ouadid-Ahidouch H & Ahidouch A (2013) K+ channels and cell cycle progression in
576 tumor cells. *Front Physiol* **4**.

577 33 Hoffmann EK, Lambert IH & Pedersen SF (2009) Physiology of cell volume regulation
578 in vertebrates. *Physiol Rev* **89**, 193–277.

579 34 Filippi-Chiela EC, Thomé MP, Bueno e Silva MM, Pelegrini AL, Ledur PF, Garicochea
580 B, Zamin LL & Lenz G (2013) Resveratrol abrogates the Temozolomide-induced G2
581 arrest leading to mitotic catastrophe and reinforces the Temozolomide-induced
582 senescence in glioma cells. *BMC Cancer* **13**, 1–13.

583 35 Behrens R, Nolting A, Reimann F, Schwarz M, Waldschütz R & Pongs O (2000)
584 hKCNMB3 and hKCNMB4, cloning and characterization of two members of the
585 large-conductance calcium-activated potassium channel beta subunit family. *FEBS*
586 *Lett* **474**, 99–106.

587 36 Contreras GF, Neely A, Alvarez O, Gonzalez C & Latorre R (2012) Modulation of BK
588 channel voltage gating by different auxiliary β subunits. *Proc Natl Acad Sci U S A*

109, 18991–18996.

37 Haworth AS & Brackenbury WJ (2019) Emerging roles for multifunctional ion channel auxiliary subunits in cancer. *Cell Calcium* **80**, 125–140.

38 Hoa NT, Ge L, Martini F, Chau V, Ahluwalia A, Kruse CA & Jadus MR (2016) Temozolomide induces the expression of the glioma Big Potassium (gBK) ion channel, while inhibiting fascin-1 expression: possible targets for glioma therapy. *Expert Opin Ther Targets* **20**, 1155–1167.

39 D'Alessandro G, Grimaldi A, Chece G, Porzia A, Esposito V, Santoro A, Salvati M, Mainiero F, Ragozzino D, Di Angelantonio S, Wulff H, Catalano M & Limatola C (2016) KCa3.1 channel inhibition sensitizes malignant gliomas to temozolomide treatment. *Oncotarget* **7**, 30781–30796.

40 Petho Z, Tanner MR, Tajhya RB, Huq R, Laragione T, Panyi G, Gulko PS & Beeton C (2016) Different expression of β subunits of the KCa1.1 channel by invasive and non-invasive human fibroblast-like synoviocytes. *Arthritis Res Ther* **18**.

41 Pethő Z, Najder K, Bulk E & Schwab A (2019) Mechanosensitive ion channels push cancer progression. *Cell Calcium* **80**, 79–90.

42 Pedersen SF, Novak I, Alves F, Schwab A & Pardo LA (2017) Alternating pH landscapes shape epithelial cancer initiation and progression: Focus on pancreatic cancer. *BioEssays* **39**.

43 Pethő Z, Najder K, Carvalho T, McMorrow R, Todesca LM, Rugi M, Bulk E, Chan A, Löwik CWGM, Reshkin SJ & Schwab A (2020) pH-channeling in cancer: How pH-dependence of cation channels shapes cancer pathophysiology. *Cancers (Basel)* **12**, 1–37.

44 Xin XF, Cheng Y, Ren J, Zhang S, Liu P, Zhao H, Huang H & Wang W (2018) The extracellular loop of the auxiliary β 1-subunit is involved in the regulation of BK Ca channel mechanosensitivity. *Am J Physiol Cell Physiol* **315**, C485–C493.

45 Dopico AM, Bukiya AN & Jaggar JH (2018) Calcium- and voltage-gated BK channels in vascular smooth muscle. *Pflugers Arch* **470**, 1271.

46 Bukiya AN, Vaithianathan T, Toro L & Dopico AM (2008) The second transmembrane domain of the large conductance, voltage- and calcium-gated potassium channel β1 subunit is a lithocholate sensor. *FEBS Lett* **582**, 673.

47 Wiemuth D, Assmann M & Gründer S (2014) The bile acid-sensitive ion channel

(BASIC), the ignored cousin of ASICs and ENaC. *Channels* **8**, 29.

48 Wang YW, Ding JP, Xia XM & Lingle CJ (2002) Consequences of the stoichiometry of Slo1 alpha and auxiliary beta subunits on functional properties of large-conductance Ca2+-activated K+ channels. *J Neurosci* **22**, 1550–1561.

49 Kuntamallappanavar G, Bisen S, Bukiya AN & Dopico AM (2017) Differential distribution and functional impact of BK channel beta1 subunits across mesenteric, coronary, and different cerebral arteries of the rat. *Pflugers Arch* **469**, 263–277.

50 Martinez-Espinosa PL, Yang C, Gonzalez-Perez V, Xia XM & Lingle CJ (2014) Knockout of the BK β2 subunit abolishes inactivation of BK currents in mouse adrenal chromaffin cells and results in slow-wave burst activity. *J Gen Physiol* **144**, 275–295.

51 Brenner R, Jegla TJ, Wickenden A, Liu Y & Aldrich RW (2000) Cloning and functional characterization of novel large conductance calcium-activated potassium channel beta subunits, hKCNMB3 and hKCNMB4. *J Biol Chem* **275**, 6453–6461.

52 Candia S, Garcia ML & Latorre R (1992) Mode of action of iberiotoxin, a potent blocker of the large conductance Ca(2+)-activated K+ channel. *Biophys J* **63**, 583–590.

53 Gonzalez-Perez V & Lingle CJ (2019) Regulation of BK Channels by Beta and Gamma Subunits. *Annu Rev Physiol* **81**, 113.